

1 **Modeling Seasonal Effects of River Flow on Water Temperatures in an Agriculturally**  
2 **Dominated California River**

3  
4  
5 **J. Eli Asarian<sup>1</sup>, Crystal Robinson<sup>2</sup>, Laurel Genzoli<sup>3</sup>**

6 <sup>1</sup>Riverbend Sciences, Eureka, CA, USA, <sup>2</sup>Quartz Valley Indian Reservation, Fort Jones, CA,  
7 USA, <sup>3</sup>Flathead Lake Biological Station and the University of Montana, Missoula, MT, USA

8 Corresponding author: J. Eli Asarian (eli@riverbendsci.com)

9  
10 **Key Points:**

- 11 • In this snowmelt and groundwater-influenced river, water temperatures stayed cool later  
12 into summer in high-flow years than low-flow years
- 13 • Statistical water temperature model predictions became more accurate when the influence  
14 of river flow was allowed to vary seasonally
- 15 • These accessible models can be applied to other rivers or streams with daily, long-term  
16 flow and water temperature records
- 17  
18  
19

## 20 **Abstract**

21 Low streamflows can increase vulnerability to warming, impacting coldwater fish. Water  
22 managers need tools to quantify these impacts and predict future water temperatures. Contrary to  
23 most statistical models' assumptions, many seasonally changing factors (e.g., water sources and  
24 solar radiation) cause relationships between flow and water temperature to vary throughout the  
25 year. Using 21 years of air temperature and flow data, we modeled daily water temperatures in  
26 California's snowmelt-driven Scott River where agricultural diversions consume most summer  
27 surface flows. We used generalized additive models to test time-varying and nonlinear effects of  
28 flow on water temperatures. Models that represented seasonally varying flow effects with  
29 intermediate complexity outperformed simpler models assuming constant relationships between  
30 water temperature and flow. Cross-validation error of the selected model was  $\leq 1.2$  °C. Flow  
31 variation had stronger effects on water temperatures in April–July than in other months. We  
32 applied the model to predict effects of instream flow scenarios proposed by regulatory agencies.  
33 Relative to historic conditions, the higher instream flow scenario would reduce annual maximum  
34 temperature from 25.2 °C to 24.1 °C, reduce annual exceedances of 22 °C (a cumulative thermal  
35 stress metric) from 106 to 51 degree-days, and delay onset of water temperatures >22 °C during  
36 some drought years. Testing the same modeling approach at nine additional sites showed similar  
37 accuracy and flow effects. These methods can be applied to streams with long-term flow and  
38 water temperature records to fill data gaps, identify periods of flow influence, and predict  
39 temperatures under flow management scenarios.

40

## 41 **Plain Language Summary**

42 Warm water temperatures threaten culturally and economically important salmon in Pacific  
43 Northwest rivers, causing chronic stress and direct mortality. Climate change and agricultural  
44 water use have reduced summer river flows in recent decades, intensifying water scarcity. Years  
45 with deep mountain snowpack and resulting high groundwater levels extend the high flow season  
46 and keep water temperatures cool through the end of July, whereas in drought years the river  
47 warms sooner. We used 21 years of river flow and air temperature data from the Scott River,  
48 California, to create computer models that simulate water temperatures. Our models allow the  
49 effect of flow on water temperatures to vary by season (i.e., stronger cooling effects in spring  
50 and summer), improving accuracy of the simulated temperatures. We used the Scott River model  
51 to simulate water temperatures under two alternative flow scenarios considered in local water  
52 management plans. Our simulations indicate that relative to current conditions, the higher flow  
53 scenario would lower the summers' highest temperatures and decrease the number of days that  
54 river temperatures exceed a biological threshold. Testing the same modeling approach at nine  
55 additional Klamath Basin sites showed similar accuracy and flow effects. Our model is freely  
56 available for public use.

57

## 58 **1 Introduction**

59 Water temperature in rivers and streams drive physical, chemical, and biological processes  
60 (Ouellet et al., 2020). Stream temperatures determine species ranges, with alterations to natural  
61 temperature regimes causing deleterious effects to native species (Wenger et al., 2011). Stream  
62 temperatures are widely altered by human activities (Webb et al., 2008). Maintaining ecological

63 integrity is a major stream temperature management goal, yet models used to predict stream  
64 temperature response to management interventions either lack predictive power or are time-  
65 consuming to develop.

66 River flow rates (i.e., discharge) are a key driver of stream temperatures through multiple  
67 mechanisms. While stream temperatures are determined by surface and streambed energy fluxes  
68 and advected heat (Caissie, 2006; Moore et al., 2005), flows mediate these effects. Higher flows  
69 generally increase water volume and thus a stream's capacity to store heat, reducing daily  
70 temperature fluctuations (Brown, 1969; Folegot et al., 2018; Meier et al., 2003; Sinokrot &  
71 Gulliver, 2000). Higher flows speed downstream transit of water, reducing the time that a parcel  
72 of water is exposed to ambient heating at a given location and increasing the influence of  
73 upstream conditions (Bartholow, 1991; Dymond J., 1984; Folegot et al., 2018). Channel  
74 geometry, including width/depth ratio, influences these effects (Dugdale et al., 2017).

75 The relationship between water temperature and flow varies through time. Seasonal changes in  
76 precipitation phase (i.e., snow and rain) affect water temperatures (Yan et al., 2021). The  
77 geographical source of water can shift seasonally, and can include tributaries, point sources,  
78 hillslopes, and alluvial aquifers, with each source having different temperatures and heating or  
79 cooling trajectories while en route to stream channels (Dugdale et al., 2017; Steel et al., 2017).  
80 Groundwater-surface water interactions and hyporheic exchange also affect temperatures  
81 (Hannah et al., 2009; Kurylyk et al., 2015). Water management, including reservoir releases,  
82 water withdrawals, and irrigation runoff can further alter temperature dynamics (Alger et al.,  
83 2021; Chandesris et al., 2019). Flow effects on water temperature are further mediated by  
84 seasonal changes to solar radiation received by the stream. Day length and solar angle, which  
85 affect topographic and riparian shading, remain consistent among years (Piotrowski &  
86 Napiorkowski, 2019; Yard et al., 2005). Other mediators of solar radiation including leaf out and  
87 leaf fall of deciduous riparian vegetation, cloud cover (Dugdale et al., 2017), water vapor, dust  
88 (Theurer et al., 1984), wildfire smoke (Asarian et al., 2020; David et al., 2018) and other aerosols  
89 follow seasonal trajectories that vary among years. Despite time-varying changes in how flow  
90 dynamics influence stream temperature, many stream temperature models do not account for  
91 these seasonal variations in the relationship between flow and stream temperatures.

92 Given stream temperature's importance and vulnerability to human alterations, water managers  
93 need tools to predict stream temperature changes associated with climate change and flow  
94 management (Gibeau & Palen, 2020; Null et al., 2017). While process-based (i.e., deterministic)  
95 models simulating stream energy budgets can have high predictive accuracy, their use is limited  
96 by extensive data input requirements (Brown, 1969; Caissie, 2006; Dugdale et al., 2017).  
97 Statistical models that use empirical relationships between stream temperature and  
98 environmental drivers require fewer input variables so are easier to implement, but for scenario  
99 prediction they are generally not considered as reliable as process-based models (Arismendi et  
100 al., 2014; Benyahya et al., 2007a; Caissie, 2006). However, statistical modeling methods have  
101 evolved, improving prediction accuracy and temporal resolution (i.e., daily) (Ouellet et al., 2020;  
102 Piotrowski & Napiorkowski, 2019). Year-round daily temperature models are especially valuable  
103 because they match the time scales used in detailed biological studies and water quality  
104 regulations (Imholt et al., 2010; Railsback et al., 2015; USEPA, 2003).

105 Statistical stream temperature models have long relied on air temperature as the primary  
106 predictor (Mohseni et al., 1998), but year-round daily models should incorporate additional  
107 mechanisms to improve accuracy and reflect physical processes (Letcher et al., 2016). Statistical

108 stream temperature models use air temperature to represent net radiative flux (Caissie 2006).  
109 Time lags between air temperatures and water temperature reflect heat exchange processes  
110 (Koch & Grünewald, 2010; Soto, 2016; Webb et al., 2003), while temporal autocorrelation  
111 acknowledges that stream temperature on a given day is in part a result of stream temperature the  
112 previous day (Benyahya et al., 2007a, 2007b, 2008; Yang & Moyer, 2020). Inclusion of flow can  
113 improve model accuracy (Piotrowski & Napiorkowski, 2019; Santiago et al., 2017; Sohrabi et  
114 al., 2017; van Vliet et al., 2011; Webb et al., 2003). The relationship between air and stream  
115 temperatures is nonlinear and differs among seasons (Arismendi et al., 2014, Caissie et al., 2001;  
116 Mohseni et al., 1998). Including time-varying effects could improve the predictive accuracy of  
117 stream temperature models across variable conditions.

118 Several methods allow seasonal variation in the relationship between environmental covariates  
119 and stream temperatures. These methods not only improve model accuracy but also identify the  
120 times when effects are strongest. While time-varying covariate effects can be represented using  
121 separate models for each season (Mohseni et al., 1998; Sohrabi et al., 2017), this may cause  
122 unnatural, abrupt changes at seasonal transitions. Time-varying coefficients, including those used  
123 in generalized additive models (GAMs) (Pedersen et al., 2019; Wood, 2017) use continuous  
124 functions that avoid these abrupt changes (Li et al., 2014; Jackson et al., 2018; Siegel & Volk,  
125 2019). While GAMs have been used in daily stream temperature modeling for single-site  
126 prediction (Boudreault et al., 2019; Coleman et al., 2021; Glover et al., 2020; Laanaya et al.,  
127 2017), spatiotemporal prediction (Jackson et al., 2018; Siegel & Volk, 2019), identifying  
128 extreme events (Georges et al., 2021), and trend assessment (Yang & Moyer, 2020), few studies  
129 have used GAMs to model seasonally varying flow effects or identify when stream temperatures  
130 are most affected by flow variation (Glover et al., 2020; Yang & Moyer, 2020). With flexible  
131 model structures and easy implementation, GAMs could be a powerful tool for predicting stream  
132 temperatures under flow management scenarios, but to our knowledge these models have not  
133 been previously used for this purpose.

134 Our objectives were to predict mean and maximum daily stream temperatures under management  
135 flow scenarios and new environmental conditions, and to identify periods when flow has the  
136 strongest influence on stream temperatures. We compared 11 GAM structures using flow, air  
137 temperature, and day of year as covariates that incorporated combinations of linear, nonlinear,  
138 and seasonally-varying effects. Our model selection and validation procedures included  
139 extrapolation tests evaluating predicted stream temperatures with flows and air temperatures  
140 outside the calibration range, designed to favor models that had enough complexity to represent  
141 the key patterns in the data, but not so complex that they overfit the data. We applied the top  
142 model to proposed management flow scenarios and extreme flow and air temperature conditions.  
143 The models are intended to be used as a tool to inform water management, making the relatively  
144 simple model structure and coding of GAMs our choice of modeling technique. We focused our  
145 analyses on the Scott River of Northern California, where low flows and high temperatures are  
146 limiting factors for coldwater fish and water managers are considering implementing regulations  
147 to protect instream flows. To demonstrate wider applicability, we evaluated similar models in  
148 nine additional sites in the Klamath River Basin.

149

## 150 2 Study Area

151 Our study area is the lower Klamath River Basin, California, USA, focusing on one large  
152 tributary—the Scott River (Figure 1). The Scott River study site is located at the outlet of Scott  
153 Valley, with a drainage area of 1,714 km<sup>2</sup>. The other nine sites are near USGS gaging stations  
154 with drainage areas ranging from 58 km<sup>2</sup> to 31,300 km<sup>2</sup> (Figure 1, Table S1). The climate is  
155 Mediterranean with precipitation occurring primarily in winter and spring as rain at low  
156 elevations and snow at higher elevations (VanderKooi et al., 2011). The human population lives  
157 primarily on private land along watercourses including Scott Valley, where irrigated agriculture  
158 dominates land use, utilizing groundwater and surface water (Foglia et al., 2018). The Scott  
159 River has no major dams or reservoirs, but there are large dams on the Klamath River and two  
160 tributaries (Shasta and Trinity rivers), influencing some study sites.

161 The Scott Valley aquifer fills during the high flows of winter rainstorms and spring snowmelt-  
162 driven runoff. As runoff recedes through summer, most surface water is diverted for irrigation  
163 and river water at the Scott Valley outlet becomes increasingly composed of groundwater from  
164 valley alluvium. Minimum flows occur in early September before rising due to fall rains (Figure  
165 2b). In late summer of drought years, portions of the Scott River have no surface flow (Tolley et  
166 al., 2019). Summer and fall river flows have declined in recent decades (Kim and Jain, 2010;  
167 Asarian and Walker, 2016) due to a combination of climate change (Drake et al., 2000) and  
168 increased groundwater withdrawals, especially since 1977 (Van Kirk and Naman, 2008). Climate  
169 change is expected to further reduce flows by decreasing snowpack and increasing irrigation  
170 demand (Persad et al., 2020).

171 Management flows have been proposed for the Scott River to protect Endangered Species Act-  
172 listed coho salmon (*Oncorhynchus kisutch*) and other coldwater salmonid fishes. These fishes'  
173 importance to local Native American tribes has led to contention over water management. River  
174 water temperatures in May–July are much cooler in high-flow years than low-flow years (Figure  
175 2), and water extraction has contributed to the Scott River being listed as impaired for water  
176 temperature under the Clean Water Act (NCRWQCB, 2005). The U.S. Forest Service has a first-  
177 priority Schedule D water right for Scott River instream flow that varies by month and day from  
178 30–200 ft<sup>3</sup>/s (0.85–5.67 m<sup>3</sup>/s) (Superior Court of Siskiyou County, 1980) (Figure 3b), but does  
179 not exercise its legal authority to curtail lower-priority water uses when flows drop below these  
180 levels. The California Department of Fish and Wildlife (CDFW) proposed interim Scott River  
181 instream flow targets that vary by month and day from 62–362 ft<sup>3</sup>/s (10.3–1.75 m<sup>3</sup>/s) (CDFW,  
182 2017) (Figure 3b), but these have no legal force.

183

## 184 3 Methods

185 At each of the 10 sites, we developed GAMs to predict daily mean stream temperature ( $T_{\text{mean}}$ )  
186 and daily maximum stream temperature ( $T_{\text{max}}$ ) using flow, air temperature, and day of year as  
187 covariates. We compared models across a range of complexity, including those with seasonally  
188 varying flow effects, to models with a constant relationship between stream temperature and  
189 flow. We selected a final model based on the best overall performance averaged across the 10  
190 sites. We then applied that model to flow management scenarios at one site—the Scott River.

## 191 3.1 Data sources and preparation

### 192 3.1.1 Water temperature and river flow

193 We obtained water temperature data from six sources (Table S1). For the Scott River site, we  
 194 used Quartz Valley Indian Reservation (QVIR) (QVIR, 2016; Asarian et al., 2020) data,  
 195 supplemented by U.S. Forest Service (USFS) (KNF, 2010, 2011) and U.S. Bureau of  
 196 Reclamation (USBR) (Smith et al., 2018) data. For the nine other sites, we used data from the  
 197 U.S. Fish and Wildlife Service (USFWS) (Manhard et al., 2018; Romberger & Gwozdz, 2018),  
 198 USFS (KNF, 2010, 2011), USBR, U.S. Geological Survey (USGS), and California Department  
 199 of Water Resources (CDWR). Following compilation, we reviewed the data and removed any  
 200 suspicious values (e.g., when there were calibration issues or probes appear to have been  
 201 exposed to air). We then calculated  $T_{\text{mean}}$  and  $T_{\text{max}}$ . For days when data were available from  
 202 multiple entities, we averaged values (Text S1). Data availability ranged from 3540–5684 days  
 203 and 16–21 years per site. We paired daily temperatures at each site with daily average  
 204 streamflow data from nearby USGS gages (Figure 1, Table S1).

### 205 3.1.2 Air temperature

206 We retrieved daily mean air temperatures for each site from the 4-km resolution gridded PRISM  
 207 dataset (Daly et al., 2008). Because stream temperatures are correlated with air temperature at  
 208 multiple time scales, we initially explored many metrics (Piotrowski & Napiorkowski, 2019). In  
 209 these initial explorations at Scott River, we found that two-day weighted air temperature ( $A_{2w}$ )  
 210 resulted in good model fits (Text S2), so we used  $A_{2w}$  for all models except one that used a  
 211 seven-day average ( $A_7$ ) to mimic Mohseni et al.’s (1998) widely-implemented model.  $A_{2w}$  is  
 212 calculated as follows, where  $A$  is mean air temperature on day  $i$ :

$$213 \quad A_{2w} = \frac{A_i + (0.5 \cdot A_{i-1})}{1.5} \quad (1)$$

214

215 To improve numerical stability, we standardized air temperature ( $^{\circ}\text{C}$ ) and flow ( $\log_{10} \text{ m}^3/\text{s}$ ) by  
 216 centering and scaling (i.e., subtracting the mean, then dividing by the standard deviation).

217

### 218 3.1.3 Flow and air temperature quantiles

219 At each site, we used smooth additive quantile regression models (Cade and Noon, 2003; Fasiolo  
 220 et al., 2020) to calculate the air temperature associated with three quantiles (0.1, 0.5, and 0.9,  
 221 equivalent to 10%, 50%, 90% exceedance probabilities) for each day of the year (Figure 3a),  
 222 using the `qgam` R package (Fasiolo et al., 2020) with a 12-knot cyclic cubic regression spline  
 223 (“cc”). We refer to the 0.1, 0.5, and 0.9 air temperature quantiles as Coolest, Typical, and  
 224 Hottest, respectively. We also derived three flow quantiles, with the 0.1 quantile representing  
 225 Lowest flows, 0.5 quantile representing Typical flows, and the 0.9 quantile representing Highest  
 226 flows (Figure 3b). These quantiles were used to generate model scenarios (Section 3.4).

227 We used similar quantile regression models at each site to categorize each date into one of nine  
 228 categories based on combinations of flow quantiles (High is  $>0.67$  quantile, Moderate is 0.33–  
 229 0.67 quantile, Low is  $<0.33$  quantile) and air temperature quantiles (Cool is  $<0.33$  quantile,

230 Moderate is 0.33–0.67 quantile, Warm is > 0.67 quantile). These categories were used to define  
231 cross-validation blocks (Section 3.3).

232

### 233 3.2 Model development and calibration

234 At each of the 10 sites, we developed 11 models of  $T_{\max}$  and  $T_{\text{mean}}$  using combinations of river  
235 flow, air temperature, and day of year (D) as covariates, including interactions (Table 1). GAMs  
236 were developed in the *mgecv* R package version 1.8-36 using the *bam* function (Wood, 2017), fit  
237 using fast restricted maximum likelihood (fREML). We also re-fit using maximum likelihood  
238 (ML) solely to obtain Bayesian information criterion (BIC) scores. Model terms were either  
239 linear coefficients or smooth non-linear functions with wiggliness determined by a smoothing  
240 penalty (Pedersen et al., 2019; Wood, 2017). We used cyclic cubic regression splines (“cc”) as  
241 the smoother for D and thin plate regression splines (“tp”) as smoothers for other covariates. To  
242 improve prediction under new conditions and avoid overfitting (Jackson et al., 2018; Siegel &  
243 Volk, 2019), we limited smoothers for air temperature and flow to a maximum of three knots,  
244 except in the one-covariate model “GAM11” where air temperature was allowed six knots. D  
245 was allowed up to six knots, except in three-dimensional tensors where it was restricted to five  
246 knots.

247 Some models included interactions between D and other covariates (i.e., flow or air temperature)  
248 to allow that covariate’s effect to vary seasonally. These interactions were either partially  
249 nonlinear or fully nonlinear. For partially nonlinear interactions, the linear slope of one variable  
250 (e.g., flow) varied as a smooth nonlinear function of D (Jackson et al., 2018, Siegel & Volk,  
251 2019). Fully nonlinear relationships between two or more variables were specified as tensor  
252 product smooths or tensor product interactions (Wood, 2017).

253 All models except “GAM11”, the simplest model structure tested, included an AR-1  
254 autocorrelation error structure and a random effect for year. We initially fit each model without  
255 an autocorrelation term, and then re-fit with an autocorrelation term, assigning a rho value based  
256 on the initial model’s lag-1 autocorrelation (Baayen et al., 2018; van Rij et al., 2019, 2020) (Text  
257 S3).

258 Since Mohseni et al.’s (1998) nonlinear logistic regression of weekly air temperature and stream  
259 temperature has been widely applied and adapted (Piotrowski & Napiorkowski, 2019), we  
260 included a GAM equivalent of it as a benchmark for comparison.  $A_7$  is the only predictor in this  
261 “GAM11” model (i.e., no flow, autocorrelation, or random effects).

262 We reviewed residual plots and autocorrelation function plots to verify assumptions. We  
263 evaluated each model’s concurvity using *mgecv*’s concurvity function.

264

### 265 3.3 Model selection and validation

266 We used cross-validation (CV) for model selection and validation because it is preferred over  
267 information theoretic approaches when prediction is paramount (Pedersen et al., 2019). We  
268 designed extrapolation CV tests to select models that performed well when applied to  
269 environmental conditions (i.e., flow and air temperature) outside the calibration range (Lute &  
270 Luce, 2017; Roberts et al., 2017). We split data into blocks based on quantiles of flow and air

271 temperature (Section 3.1.3), withheld one block, and fit the model using the remaining block  
272 (Figure 4). We compared predictions for the withheld block against the measured data using root  
273 mean squared error (RMSE). These dual-variable differential split-sample tests (Klemeš, 1986)  
274 extrapolate not only into new combinations of flow and air temperature but also into new ranges  
275 of both individual variables.

276 We selected the final model by averaging all 40 RMSE values from extrapolation tests (10 sites  
277  $\times$  2 extrapolation tests  $\times$  2 parameters [ $T_{\max}$  and  $T_{\text{mean}}$ ]) and choosing the model with lowest  
278 mean RMSE. We selected the same model structure for  $T_{\max}$  and  $T_{\text{mean}}$  (rather than optimizing  
279 separately) so predictions for both metrics could be used together. We present BIC scores to  
280 compare our extrapolation-based model selection to more commonly applied model selection  
281 methods. To facilitate comparisons to previous studies, we also use leave-one-year-out (LOYO)  
282 CV where data were split into annual blocks and then treated similarly to the extrapolation tests  
283 (i.e., steps repeated for each year: year withheld, model refit using remaining data, and  
284 predictions compared to withheld data). We assessed the relative importance of individual model  
285 terms by comparing performance among models with and without individual predictors and/or  
286 interactions.

287

## 288 3.4 Model scenarios assessing management effects and timing of flow importance

### 289 3.4.1 All sites

290 To assess the seasonal response of stream temperatures to variation in flow and air temperatures,  
291 we applied our selected model to scenarios representing differing air temperatures and flows  
292 (Table 2, Figure 3). We ran nine “quantile air temperature” scenarios representing combinations  
293 of three air temperature inputs (0.1, 0.5, and 0.9 quantiles) and three flow inputs (0.1, 0.5, and  
294 0.9 quantiles) (Section 3.1.3) for each site. Replication is sparse for the co-occurrence of extreme  
295 quantiles of both air temperature and flow (e.g., mean 4.9 days of record per month and site with  
296 flow  $\leq 0.1$  quantile and air temperature  $\geq 0.9$  quantile); however, ample data are available in  
297 nearby quantiles (e.g., mean 19.1 days per month and site with flow  $\leq 0.2$  quantile and air  
298 temperature  $\geq 0.8$  quantile) (Figure S1).

299

### 300 3.4.2 Scott River

301 At Scott River only, six additional scenarios were run that paired the three quantile air  
302 temperatures with the USFS water right and CDFW flow criteria (Section 2) as flow inputs  
303 (Table 2, Figure 3). The CDFW and USFS flows are aligned with extreme drought conditions in  
304 April and May (0.1 quantile) and high flows in August and September (0.5 to 0.9 quantile).

305 We also applied our selected model to “observed air temperature” scenarios that pair observed  
306 air temperatures for dates 1998–2020 with eight flow conditions for the Scott River: observed  
307 USGS flows, the five flows from the “quantile air temperature” scenarios (Lowest, Typical,  
308 Highest, USFS, and CDFW), and two additional scenarios in which the CDFW and USFS flows  
309 were replaced by observed USGS flows on dates when the observed flows were higher than the  
310 management flows (Table 2). Using observed air temperatures instead of quantile air  
311 temperatures provides more realistic predictions because air temperatures fluctuate from day to

312 day (Figure 2a), instead of remaining near the same quantile like flow does during May–  
313 September recession. We summarized the results of each “observed air temperature” scenario by  
314 calculating: 1) annual maximum temperature, 2) first and last day each year in which water  
315 temperatures exceed 22 °C, and 3) the annual degree days exceedance of 22 °C, calculated by  
316 subtracting 22 from all  $T_{\max}$  and summing all positive values. We chose 22 °C as an indicator of  
317 biological effects on juvenile salmonids, based on geographically proximal studies (Brewitt and  
318 Danner, 2014; Sutton et al., 2007; Sutton & Soto, 2012) (Text S4).  
319  
320

## 321 **4 Results**

### 322 4.1 Model selection and validation

323 In extrapolation CV of the 11 models (Table 1), GAM7 had the lowest all-site mean RMSE ( $T_{\max}$   
324 1.13 °C,  $T_{\text{mean}}$  1.00 °C), as well as the lowest RMSE for Scott River ( $T_{\max}$  1.20 °C,  $T_{\text{mean}}$  1.00  
325 °C), so was selected as our final model (Figure 5). GAM7 features nonlinear smoothers for day  
326 of year (D), two-day weighted air temperature ( $A_{2w}$ ), and flow (Q); a nonlinear smoother of D  
327 interacted with linear Q (i.e., linear slope of Q varies by D); and a nonlinear smoother of D  
328 interacted with linear  $A_{2w}$  (Table 1, Figure S3, Figure 6). GAM7 has intermediate complexity,  
329 with 12.6 effective degrees of freedom for fixed effects ( $\text{edf}_F$ ) for Scott River  $T_{\max}$ , compared to  
330 23.6 for the most complex model (GAM1), and 5.8 for the least complex model (GAM11) (Table  
331 1).

332 Extrapolation CV showed that at all sites, including Scott River, models with seasonally varying  
333 flow effects had much higher accuracy than models lacking that feature (Figure 5). For example,  
334 for  $T_{\max}$ , all-site RMSE was 1.13–1.17 °C for models with seasonally-varying flow effects  
335 (GAM1–GAM8) and 1.66 °C for GAM9 that lacked seasonally varying flow. Models lacking  
336 flow (i.e., containing only D or  $A_{2w}$ ) performed the worst, with all-site RMSE values of 1.72 °C  
337 and 2.21 °C for GAM10 and GAM11, respectively, for  $T_{\max}$ . GAM7’s combination of a  
338 nonlinear smoother for flow and a partially nonlinear interaction of flow and D represented flow  
339 effects well, given that the additional complexity of tensors (fully nonlinear interactions of flow  
340 and D) in GAM1–GAM5 did not substantially improve model performance at most sites. Models  
341 interacting flow and air temperature (i.e., GAM1 and GAM4) did not outperform GAM7 which  
342 lacked this interaction.

343 BIC scores (Figure S4) largely corroborate the extrapolation CV results identifying the  
344 importance of seasonally varying flow effects. Of eight models with seasonally varying flow  
345 effects, the most complex model (three-way tensor GAM1) had the worst overall (averaged  
346 across all sites) BIC score, but intermediate extrapolation CV RMSE. Averaging BIC ranks  
347 across sites, our extrapolation CV-selected model, GAM7, had the best BIC ranks for both  $T_{\max}$   
348 and  $T_{\text{mean}}$  (Figure S4); however, at many individual sites including Scott River, other models had  
349 better BIC scores (Figure S4, Table 1).

350 Scott River GAM7 LOYO CV predicted overall seasonal patterns in measured  $T_{\max}$  for dates  
351 stratified into combinations of differing quantiles of air temperatures and flows. RMSE was  
352 higher for dates with low (<0.33 quantile) flows (Figure S2c).  $T_{\max}$  Scott River GAM7  
353 extrapolation CV prediction accuracy was only slightly lower than LOYO CV prediction  
354 accuracy when averaged over the entire year (i.e., RMSE 1.20 °C vs. 1.18 °C, Figure 5), but

355 were biased low during May and June during high ( $>0.67$  quantile) flows, having only been  
356 calibrated with data from the low-flow and moderate-flow quantile (Figure S5). Complete time  
357 series of Scott River measured and LOYO CV  $T_{\max}$  and  $T_{\text{mean}}$  for all years are shown in Figures  
358 S6–S7.

359

#### 360 4.2 Model scenarios assessing management effects and timing of flow importance

361 Water temperature predictions under quantile air temperature scenarios on the Scott River using  
362 our selected model (GAM7) showed water temperatures responded to changes in flow across all  
363 quantiles of air temperature, consistent with measured data (Figure S2). Cooling effects of flow  
364 followed a seasonal pattern, rising in March to reach maximum effect size on 15 June ( $7.7\text{ }^{\circ}\text{C}$  for  
365  $T_{\max}$  and  $5.5\text{ }^{\circ}\text{C}$  for  $T_{\text{mean}}$ ), then diminishing to near zero by early September (Figure 7).  
366 Consistent with measured data (Figure S2), modeled annual maximum water temperatures  
367 occurred later in the season in high-flow conditions (i.e., late July or early August) than in low-  
368 flow conditions (i.e., early/mid-July) (Figure 7).

369 Timing and magnitude of flow effects varied among the 10 Klamath Basin sites, but generally  
370 followed a similar seasonal trend of flow having the strongest cooling effects in April–July, less  
371 cooling effects in March and August, and warming effects in November through February  
372 (Figure 8). Cooling effects of flow were strongest at Scott River and weakest at Shasta River.

373 The Scott River “observed air temperature” scenarios, which paired observed air temperatures  
374 with eight flow scenarios, demonstrated how flow variation influences stream temperature timing  
375 and magnitude. The lowest flow scenario (0.1 quantile) had annual maximum temperatures  $3.3$   
376  $^{\circ}\text{C}$  warmer than the highest flow scenario (0.9 quantile) (Figure 9a), and first reached  $22\text{ }^{\circ}\text{C}$  48  
377 days earlier (Figure 9c). The last day with temperatures  $>22\text{ }^{\circ}\text{C}$  differed by only 2 days (Figure  
378 9d). The observed scenario had the most interannual variation in annual maximum temperature  
379 (Figure 9a) and timing of exceedances of  $22\text{ }^{\circ}\text{C}$  (Figure 9c,d), because it included very low flows  
380 and very high flows. Predicted temperature responses to the CDFW and USFS flow scenarios are  
381 complex and depend on how the flows are implemented. If implemented as bypass flows, above  
382 which all additional water is diverted, then temperatures reached  $22\text{ }^{\circ}\text{C}$  *earlier* than the observed  
383 flow scenario by 4 days for the CDFW flows and 13 days for USFS flows (Figure 9c and Figure  
384 S8) because these management flows are lower than observed flows in May and June (Figure 3).  
385 However, in the scenarios where the CDFW and USFS flows were replaced by observed USGS  
386 flows on dates when the observed flows were higher than the management flows, then predicted  
387 temperatures reached  $22\text{ }^{\circ}\text{C}$  *later* than the observed scenario by 4 days with CDFW flows and 2  
388 days with USFS flows. In addition, the number of years with exceedances of  $22\text{ }^{\circ}\text{C}$  prior to 23  
389 June were reduced from 7 to 0 (Figure 9c) because CDFW flows were higher than observed  
390 flows in drought years. Due to higher July and August flows, annual maximum water  
391 temperatures were  $1.0\text{--}1.1\text{ }^{\circ}\text{C}$  cooler in the CDFW scenarios than the observed flow scenario  
392 (Figure 9a). Differences in annual degree-days exceedance of  $22\text{ }^{\circ}\text{C}$  between scenarios (Figure  
393 9b) were similar to annual maximum temperature.

394

## 395 5 Discussion

396 At all 10 sites, models with seasonally varying flow effects substantially outperformed models  
397 with a constant relationship between stream temperature and flow, indicating that the influence  
398 of flow changes throughout the year. Models containing only air temperature performed  
399 particularly poorly because they did not include flow as a covariate, while models with a linear  
400 effect of flow had intermediate accuracy. Flow had the strongest effect on water temperatures in  
401 April–July. The highest Scott River management flow evaluated would substantially decrease  
402 exceedances of 22 °C and reduce annual water temperature maximums.

### 403 5.1 Model selection and performance

404 Model accuracy of our top model and similar model structures were high for both  $T_{\max}$  and  $T_{\text{mean}}$ .  
405 For  $T_{\text{mean}}$ , our selected model's LOYO CV RMSE ranged from 0.80–1.17 °C at 10 sites (Figure  
406 5), better than the 0.75–1.75 °C RMSE in Mohseni-based models at 14 sites within our study  
407 area (Manhard et al., 2018). In addition to outperforming other models applied within our study  
408 area, our selected  $T_{\text{mean}}$  model also had better LOYO CV RMSE than most single-station year-  
409 round daily statistical models from around the world (all-site average model validation RMSE  
410 for each analysis's best performing class of models: Ahmadi-Nedushan et al. [2007] 0.51 °C,  
411 Boudreault et al. [2019] 1.45 °C, Coleman et al. [2021] 1.3 °C, Koch and Grünwald [2010] 1.25  
412 °C, Laanaya et al. [2017] 1.44 °C, Letcher et al. [2016] 1.16 °C, Sohrabi et al. [2017] 1.25 °C,  
413 van Vliet et al. [2011] 1.8 °C, and Soto et al. [2016] 1.20 °C). Our high model accuracy was  
414 achieved despite using PRISM air temperatures instead of local measurements—favoring ease of  
415 replicability.

416 GAMs were a useful modeling approach because they represented the nonlinear relationships  
417 and interactions between stream temperature and covariates. Our approach used >15-year  
418 calibration datasets spanning environmental conditions (i.e., hot and cool air temperatures and  
419 high and low flows). We prevented overfitting by restricting the number of knots in GAM  
420 smoothers (Section 3.2), basing model selection on extrapolation tests that evaluate prediction  
421 under expanded ranges of covariates (Section 3.3), and confirming that covariate responses and  
422 interactions matched scientific hypotheses regarding underlying physical processes (Section 5.3).  
423 Our selected model, GAM7, represented flow with two terms—a nonlinear smoother and a  
424 partially nonlinear interaction between flow and day of year—whose combined effects (Figure 6)  
425 provided enough flexibility for accurate predictions without overfitting. This two-term structure  
426 incrementally improves upon previous methods for representing flow effects, with GAM7's  
427 overall extrapolation CV RMSE 0.04 °C better than GAM6, the model with a simpler flow  
428 effects structure nearly identical to Glover et al. (2020). Consistent with warnings from Siegel &  
429 Volk (2019), tensors (fully nonlinear interactions) were too flexible and did not perform as well  
430 as GAM7 when applied to conditions differing from the calibration dataset (i.e., extrapolation  
431 tests), although tensor models still outperformed models without seasonally varying flow effects.

432

### 433 5.2 Magnitude and timing of flow effects on water temperature

434 Consistent with physical expectations, our results corroborate previous findings from northern  
435 temperate rivers that during seasons when air temperatures are typically high and flows are  
436 typically low (i.e., summer in our study area), lower flows are often temporally correlated with  
437 higher stream temperatures (Arora et al., 2016; Isaak et al., 2017; Luce et al., 2014; Neumann et

438 al., 2003), and flow more strongly affects  $T_{\max}$  than  $T_{\text{mean}}$  (Asarian et al., 2020; Gu and Li, 2002;  
439 Gu et al., 1998). In our study streams, high flows had a strong cooling effect on stream  
440 temperatures in April–July, but less influence during other months. Multiple linear regression  
441 (MLR) models using monthly flow and air temperature at 239 Northwestern USA sites not  
442 regulated by dams (Isaak et al., 2018) and spatial stream network models for eight regions of the  
443 Western USA (FitzGerald et al., 2021) showed monthly timing and direction of flow effects on  
444 stream temperatures (Figures S9–S10) similar to our results (Figure 8b), with the exception of  
445 similar cooling in April and August whereas our models show weaker cooling in August than in  
446 April. Monthly MLR modeling in 17 sites in Canada’s Frasier River Basin found flow-mediated  
447 cooling effects on summer water temperatures were stronger in July than August and weakest in  
448 September (Islam et al., 2019). In Poland, where inter-season flow differences are less  
449 pronounced than in our study area, high flows were correlated with cooler water temperatures in  
450 April–September, with the strongest relationships occurring in July–September at mountainous  
451 snowmelt-fed rivers (Wrzesiński and Graf, 2022). An Eastern USA river study using a daily  
452 year-round GAM found that water temperature decreased with increased flow from April  
453 through mid-October (Yang & Moyer, 2020). Previous studies evaluating year-round changes in  
454 the relationship between stream temperature and flow generally used monthly time steps. Our  
455 daily model provides a more nuanced understanding of seasonal dynamics by allowing this  
456 relationship to change smoothly at sub-monthly time scales, facilitating identification of changes  
457 within a month, as well as the rate of change.

458 Flow-induced cooling in snowmelt-dominated rivers is common. Process-based modeling of a  
459 Sierra Nevada river indicated early summer stream temperatures up to 16 °C cooler in a record  
460 wet year relative to a dry year (Null et al., 2013). In steep Alaskan streams, average summer  
461 stream temperatures were 3–5 °C cooler in high-snowpack years than low-snowpack years (Cline  
462 et al., 2021). In the conterminous USA, including flow as a covariate improved daily stream  
463 temperature predictions over air temperature only models in April–August, but only in  
464 snowmelt-dominated streams (Sohrabi et al., 2017). Stronger flow effects occurred in inland  
465 regions than coastal regions of the Western USA (Figure S10) (FitzGerald et al., 2021),  
466 consistent with a greater percent of precipitation falling as snow (Klos et al., 2014). Climate  
467 change studies have not parsed the separate influences of hydrology and air temperature on  
468 stream temperature, but in snowmelt-dominated areas of western North America, predictions for  
469 disproportionate spring and summer stream temperature warming are nearly ubiquitous and  
470 attributed to snowpack declines causing lower flows in those seasons (Caldwell et al., 2013;  
471 Crozier et al., 2020; Ficklin et al., 2014; Leach & Moore, 2019; Lee et al., 2020; Luo et al., 2013;  
472 Null et al., 2013).

473

### 474 5.3 Model correspondence to physical mechanisms

475 We used air temperature and flow as the major predictors in our model, recognizing that these  
476 predictors represent many processes that collectively determine stream temperatures. Air  
477 temperature is not the most important component of stream heat budgets (Johnson, 2004;  
478 Dugdale et al., 2017), but it has high predictive power because it is correlated with net radiative  
479 flux, a key driver of stream heat budgets (Caissie 2006). Air temperature data resulted in high  
480 model accuracy in our study, and are widely attainable unlike radiative fluxes.

481 The effects of flow on stream temperature vary throughout the year in response to the physical  
482 mechanisms affecting stream energy balances. High flows speed downstream transit of water and  
483 provide increased thermal mass that resists heating (or cooling). While flow has strong effects on  
484 water temperature in April–July in our study area, its effects are substantially weaker—though  
485 still present—in August. High flow can exert a dominant influence on water temperature, but this  
486 influence wanes as flow recedes, leading to progressively greater influence of solar radiation and  
487 air temperature. The relationship between flow and water temperature in our top-performing  
488 model is nonlinear and varies with day. Marginal effects of decreasing flow diminish as flow  
489 approaches  $0 \text{ m}^3/\text{s}$  (Figure 6). At Scott River, August flows were much lower than July (Figure 2,  
490 Figure 6), and by 15 August were always below  $2.6 \text{ m}^3/\text{s}$  ( $92 \text{ ft}^3/\text{s}$ ). These low August flows have  
491 shallow water depth, low thermal mass, and slow transit times resulting in residence time  
492 sufficient for water to heat up to equilibrium temperature (Bogan et al., 2003; Nichols et al.,  
493 2014; Tague et al., 2007). During hot, dry conditions such occurs in our study area during  
494 summer, evaporative cooling limits how high stream temperatures can rise even when flows are  
495 extremely low (Mohseni & Stefan, 1999; Mohseni et al., 1998; Shaw et al., 2017). Wildfire  
496 smoke could also reduce warming of August stream temperatures (David et al., 2018).  
497 Widespread fire is more likely during drought conditions (Westerling, 2016), suggesting  
498 potential for smoke to confound low flow effects on temperature by decreasing solar radiation.  
499 We did not include smoke in our models because the data are difficult to process and we wanted  
500 easily replicable methods, but smoke effects on stream temperatures peaked in August in our  
501 study area (Asarian et al., 2020). With less solar radiation and cooler air temperatures than earlier  
502 months,  $T_{\text{max}}$  is almost always less than  $22 \text{ }^\circ\text{C}$  at Scott River by early September regardless of  
503 flow (Figure 7). In October–November, a period of hydrologic transition when precipitation ends  
504 seasonal baseflow recession, flows had little influence over stream temperature (Figure 8), but  
505 Scott River and two other sites had weak, modal flow-temperature relationships (i.e., highest  
506 water temperatures at moderate flows) (Text S5).

507 Groundwater contributes to the relationship between flow and stream temperature at our Scott  
508 River site, as it does in many rivers (Briggs et al., 2018; Isaak et al., 2017; Kelleher et al., 2012;  
509 Mayer, 2012; Nichols et al., 2014). Thermal infrared imagery, field measurements (NCRWQCB,  
510 2005), and a groundwater model (Tolley et al., 2019) confirm that the 10 km of river directly  
511 upstream of our study site are a gaining reach where valley constriction forces substantial  
512 groundwater into the Scott River, a common phenomenon at the outlet of alluvial valleys  
513 (Stanford and Ward, 1992). Scott River flows are driven by a mix of valley groundwater  
514 dynamics and snowmelt-driven mountain runoff (Foglia et al., 2013; Van Kirk and Naman,  
515 2008). As mountain runoff recedes and tributaries are almost fully diverted for irrigation, the  
516 relative contribution of groundwater to surface flow at the valley outlet increases over the  
517 summer and becomes dominant (NCRWQCB, 2005). Sediments underlying the river and its  
518 tributaries have high hydraulic conductivity, so groundwater and surface water are strongly  
519 connected (Tolley et al., 2019). During the May–September recession period when temperatures  
520 are of greatest biological concern, flows are related to aquifer levels, and the relative proportions  
521 of valley outlet flow derived from mountain runoff and groundwater are well-predicted by flow  
522 and day of year. Thus, even though these two sources have different temperatures and our model  
523 does not explicitly differentiate them, the model performs well because the interaction of flow  
524 and day of year implicitly characterizes these dynamics adequately. Scenarios from a short-term  
525 process-based surface water model predicted doubling groundwater-derived flow would cool 30  
526 July 2003 Scott River  $T_{\text{max}}$  by  $2 \text{ }^\circ\text{C}$ , and a 50% reduction of groundwater-derived flow would

527 warm temperatures by 2 °C (NCRWQCB, 2005). For comparison, applying our model to  
528 scenarios doubling or halving the 3.03 m<sup>3</sup>/s (107 ft<sup>3</sup>/s) gaged flow for that same date predicts  
529 T<sub>max</sub> 1.0 °C cooler or 0.7 °C warmer, respectively.

530 Statistical models typically require many fewer variables as data inputs than process-based  
531 models do, so are often much simpler to develop (Caissie, 2006; Ouellet et al., 2020); however,  
532 this ease has tradeoffs. For example, our model does not differentiate between specific sources of  
533 inflows, which may have quite different temperature influences, nor how alternative  
534 management scenarios would spatially and temporally alter those inflows. If fundamental  
535 characteristics of valley hydrology (i.e., management or climate) changed dramatically, model  
536 accuracy could suffer. Similarly, applying the model to covariate combinations beyond those  
537 used in calibration will degrade predictive accuracy (Section 5.5). To avoid overly complex  
538 models that overfit calibration data, we used extrapolation tests to favor selection of simpler  
539 more generalizable models. Our model does not incorporate longer-term (e.g., annual to decadal)  
540 variation in air temperature that affects groundwater temperatures and precipitation phase (e.g.,  
541 snow or rain), so may underestimate responses relative to predictions from integrated process-  
542 based models (Leach & Moore 2019).

543

#### 544 5.4 Biological implications

545 Higher Scott River flows extend the period when cool water habitat is available (Figure 9),  
546 giving juvenile salmonids additional time to migrate downstream and reduce thermal stress for  
547 fish that rear in the Scott River through the entire summer. Climate change will likely continue to  
548 reduce snowpack and summer flows (Persad et al., 2020), increasing duration of detrimentally  
549 warm temperatures. Mean diel range in June–August exceeds 5 °C, providing hours daily with  
550 temperatures <22 °C even when T<sub>max</sub> exceeds 22 °C. Salmonids can potentially persist by using  
551 thermal refugia where cool tributaries, groundwater, or hyporheic flow enters the river during  
552 hotter hours and then forage in the mainstem when temperatures are cooler (Brewitt and Danner,  
553 2014; Sutton et al., 2007; Sutton & Soto, 2012). However, substantial portions of the Scott River  
554 and tributaries lack surface flow during summer, especially in dry years, reducing habitat  
555 connectivity.

556

#### 557 5.5 Applications and management implications

558 These models can be used not only to identify the seasonally varying influence of flow, but also  
559 to predict future stream temperatures based on managed flow recommendations and to impute  
560 missing data. Instream flow management frameworks are evolving (Mierau et al., 2017; Poff et  
561 al., 2017; Yarnell et al., 2020) and accurate stream temperature models provide a valuable tool to  
562 predict management outcomes.

563 Our modeling approach could facilitate water managers' ability to include stream temperature as  
564 a management target in areas that do not currently have operational process-based models. For  
565 example, Siskiyou County is developing a groundwater sustainability plan for the Scott Valley  
566 (Foglia et al., 2018). The current groundwater model does not simulate water temperatures  
567 (Tolley et al., 2019). Our model can be used to predict effects of flow on Scott River  
568 temperatures, including the CDFW and USFS flow thresholds under consideration, and could

569 inform state agencies' development of new flow objectives. The CDFW and USFS flows were  
570 both predicted to cool maximum annual temperatures relative to current conditions, but  
571 improvements would be greater with the higher CDFW flows (Figure 9). We caution that while  
572 the CDFW and USFS flows are higher than typical observed flows in late summer and early fall,  
573 for March to early June they represent extreme drought conditions that could cause earlier  
574 exceedances of 22 °C (Figure 2b). Surface water diversions for in lieu recharge (switching  
575 irrigation source from groundwater to surface water) or managed aquifer recharge (Dahlke et al.,  
576 2018; Foglia et al., 2013) should not use the CDFW and USFS flows to guide maximum  
577 diversion rates, but instead be tailored to reduce deleterious effects on instream habitat including  
578 temperatures, such as ceasing diversions by 1 June, the first date when measured (Figure 2) and  
579 modeled temperatures (Figure 9) reach 22 °C.

580 As with any statistical model, prediction accuracy will degrade when applied to conditions more  
581 extreme than those present in the calibration dataset. Our selected model interacts day of year  
582 with flow and air temperature, so extrapolation caution applies not just to the range of individual  
583 variables but also their combined distributions. Our calibration dataset includes a wide range of  
584 hydrologic conditions, but no years without surface water diversions or groundwater pumping  
585 because those activities occur every year. Streamflow depletion from groundwater pumping is  
586 greater in dry years than wet years (Foglia et al., 2013). Simulated total valley-wide streamflow  
587 depletion peaks around 150,000 m<sup>3</sup>d<sup>-1</sup> (60 ft<sup>3</sup>/s) in July–August (Foglia et al., 2013), exceeding  
588 streamflow in dry years. Our model should be suitable for modeling dry years for scenarios with  
589 reduced pumping and/or diversions, which would presumably have flows similar to existing wet  
590 years (and hence are within the range of calibration flows); however, in wet years such scenarios  
591 would likely exceed the range of calibration flows and therefore be subject to more uncertainty.  
592 Future application to scenarios with flows higher than observed should be interpreted with  
593 appropriate caveats.

594 Flow records are typically less available than water temperature records, so may constrain where  
595 our modeling approach can be applied. However, if site-specific flows were not available, data  
596 from a nearby site could be used if they were likely to be highly correlated (i.e., similar  
597 watershed characteristics). We did not systematically explore that issue, but the one site (South  
598 Fork Trinity River) where we used flows from an upstream station had prediction accuracy  
599 similar to the other nine sites (Figure 5). In addition, although our modeling approach should  
600 work well with records shorter than the >15-year datasets we used, we recommend further  
601 research to determine the minimum required period of record.

602 These models can also be used to fill gaps in stream temperature data records needed for other  
603 analyses (Glover et al., 2020). Their high accuracy suggests they would compare well with  
604 imputation methods used in recent daily year-round stream temperature analyses (Isaak et al.,  
605 2020; Johnson et al., 2021).

606

## 607 **6 Conclusions**

608 Long-term daily stream temperature datasets enabled development of generalized additive  
609 models (GAMs) that include nonlinear and seasonally varying effects of flow and air  
610 temperature on stream temperature. Cross-validation indicated these models had higher accuracy  
611 than models that did not account for seasonally variable effects of flow, providing evidence that

612 flow is important in controlling stream temperatures and that the influence of flow is variable  
613 through time. Results from these models indicated that high river flow had a strong cooling  
614 effect on river temperatures during April through July at 10 sites in the Klamath Basin of  
615 California, corroborating similar findings from western North America.

616 Results from extrapolation cross-validation tests show that our selected model is robust in  
617 estimating stream temperatures under environmental conditions moderately outside of the range  
618 of conditions used to train the model (although see cautions in Section 5.5). We applied the  
619 model to instream flow management scenarios proposed by regulatory agencies at our focal  
620 study site, the Scott River, finding that these scenarios would improve stream temperatures.  
621 Relative to historic conditions, the higher instream flow scenario would reduce annual maximum  
622 temperature from 25.2 °C to 24.1 °C, reduce annual exceedances of 22 °C (a cumulative thermal  
623 stress metric) from 106 to 51 degree-days, and delay onset of water temperatures >22 °C during  
624 some drought years.

625 These models contribute to an emerging body of work demonstrating the use of GAMs for  
626 predicting daily river temperatures. Our models are easy to implement and improve prediction  
627 accuracy of stream temperature responses to flow changes over models without seasonally  
628 variable effects of flow, providing tools that managers can use to select flow solutions most  
629 likely to protect species and ecosystems. The models are implemented in the R software  
630 environment with publicly accessible code. Testing at 10 streams in our study region indicated  
631 that models with seasonally variable flow effects had high prediction accuracy across all streams,  
632 suggesting that these models have broad applicability over a range of stream types. Our selected  
633 model, GAM7, incrementally improves upon previous methods for representing flow effects.  
634 Model applications include those explored here (i.e., scenario prediction and identifying periods  
635 of flow importance), as well as filling gaps in temperature time series. We suggest that GAM7,  
636 as well as similar model structures (i.e., GAM6, GAM8) will perform well across a range of  
637 streams. Model validation procedures, including extrapolation-based methods when models are  
638 applied to new data, should be conducted to test model accuracy at new sites and for datasets of  
639 variable periods of record.

640

#### 641 **CRedit authorship contribution statement**

642 J.E.A.: Conceptualization, Data curation, Methodology, Formal analysis, Visualization, Writing  
643 – original draft, Writing – review & editing. C.R.: Conceptualization, Investigation, Data  
644 curation, Funding acquisition, Project administration, Writing - review & editing. L.G.: Writing -  
645 review & editing.

646

#### 647 **Acknowledgments**

648 The Klamath Tribal Water Quality Consortium (Karuk Tribe, Yurok Tribe, Hoopa Valley Tribe,  
649 Quartz Valley Indian Reservation, and Resighini Rancheria) supported J.E.A. and L.G. using  
650 funds provided by the U.S. Environmental Protection Agency, Region 9. Maija Meneks (KNF)  
651 and Callie McConnell (USFS Corvallis) provided the USFS water temperature data. Isaiah  
652 Williams, Alex Case, Sean Ryan and Marla Bennett (QVIR) assisted with data collection. Taylor  
653 Daley (USFWS Arcata) provided USFWS water temperature data. Daniel Isaak and Sara John

654 provided data from Isaak et al. (2018) and FitzGerald et al. (2021), respectively. WRR editors  
 655 and reviewers provided comments that substantially improved this manuscript.

656

### 657 **Data Availability Statement**

658 All input and output data and codes are archived in the online repository HydroShare (Asarian et  
 659 al., 2022, <http://www.hydroshare.org/resource/a6653e2919964f9b840ec0340d86e11c>). USBR  
 660 and USGS stream temperature data (Smith et al., 2018) are also available at  
 661 [https://or.water.usgs.gov/cgi-bin/grapher/graph\\_setup.pl?site\\_id=11519500](https://or.water.usgs.gov/cgi-bin/grapher/graph_setup.pl?site_id=11519500) and  
 662 [https://cdec.water.ca.gov/dynamicapp/staMeta?station\\_id=RCL](https://cdec.water.ca.gov/dynamicapp/staMeta?station_id=RCL). CDWR stream temperature data  
 663 are also available are available at  
 664 <https://wdl.water.ca.gov/WaterDataLibrary/StationDetails.aspx?Station=F3410000>. Gridded  
 665 PRISM air temperature data (Daly et al., 2008) are also available at:  
 666 <https://prism.oregonstate.edu/explorer/>.

667

### 668 **References**

- 669 Alger, M., Lane, B. A., & Neilson, B. T. (2021). Combined influences of irrigation diversions  
 670 and associated subsurface return flows on river temperature in a semi-arid region. *Hydrological*  
 671 *Processes*, 35(8), e14283. <https://doi.org/10.1002/hyp.14283>
- 672 Amodio, S., Aria, M., & D'Ambrosio, A. (2014). On concurvity in nonlinear and nonparametric  
 673 regression models. *Statistica*, 74(1), 85–98. <https://doi.org/10.6092/issn.1973-2201/4599>
- 674 Arismendi, I., Safeeq, M., Dunham, J. B., & Johnson, S. L. (2014). Can air temperature be used  
 675 to project influences of climate change on stream temperature? *Environmental Research Letters*,  
 676 9(8), 084015. <https://doi.org/10.1088/1748-9326/9/8/084015>
- 677 Arora, R., Tockner, K., & Venohr, M. (2016). Changing river temperatures in northern Germany:  
 678 Trends and drivers of change. *Hydrological Processes*, 30(17), 3084–3096.  
 679 <https://doi.org/10.1002/hyp.10849>
- 680 Asarian, J.E., Cressey, L., Bennett, B., Grunbaum, J., Cyr, L., Soto, T., & Robinson, C. (2020).  
 681 Influence of snowpack, streamflow, air temperature, and wildfire smoke on Klamath Basin  
 682 stream temperatures, 1995-2017. Eureka, CA: Riverbend Sciences.  
 683 <https://doi.org/10.13140/RG.2.2.22934.47681>
- 684 Asarian, J. E., Robinson, C., & Genzoli, L. (2022). Data and codes for: Modeling seasonal  
 685 effects of river flow on water temperatures in an agriculturally dominated California river.  
 686 HydroShare, <http://www.hydroshare.org/resource/a6653e2919964f9b840ec0340d86e11c>
- 687 Asarian, J. E., & Walker, J. D. (2016). Long-term trends in streamflow and precipitation in  
 688 Northwest California and Southwest Oregon, 1953-2012. *Journal of the American Water*  
 689 *Resources Association*, 52(1), 241–261. <https://doi.org/10.1111/1752-1688.12381>
- 690 Baayen, R. H., van Rij, J., de Cat, C., & Wood, S. (2018). Autocorrelated errors in experimental  
 691 data in the language sciences: some solutions offered by generalized additive mixed models. In  
 692 D. Speelman, K. Heylen, & D. Geeraerts (Eds.), *Mixed-Effects Regression Models in Linguistics*  
 693 (pp. 49–69). Springer International Publishing. [https://doi.org/10.1007/978-3-319-69830-4\\_4](https://doi.org/10.1007/978-3-319-69830-4_4)

- 694 Bartholow, J. M. (1991). A modeling assessment of the thermal regime for an urban sport  
695 fishery. *Environmental Management*, 15(6), 833. <https://doi.org/10.1007/BF02394821>
- 696 Benyahya, L., Caissie, D., St-Hilaire, A., Ouarda, T. B. M. J., & Bobée, B. (2007a). A review of  
697 statistical water temperature models. *Canadian Water Resources Journal / Revue Canadienne*  
698 *Des Ressources Hydriques*, 32(3), 179–192. <https://doi.org/10.4296/cwrj3203179>
- 699 Benyahya, L., St-Hilaire, A., Ouarda, T. B. M. J., Bobée, B., & Ahmadi-Nedushan, B. (2007b).  
700 Modeling of water temperatures based on stochastic approaches: Case study of the Deschutes  
701 River. *Journal of Environmental Engineering and Science*, 6(4), 437–448.  
702 <https://doi.org/10.1139/s06-067>
- 703 Benyahya, L., St-Hilaire, A., Ouarda, T., Bobee, B., & Dumas, J. (2008). Comparison of non-  
704 parametric and parametric water temperature models on the Nivelles River, France. *Hydrological*  
705 *Sciences Journal*, 53(3), 640–655.
- 706 Bogan, T., Mohseni, O., & Stefan, H. G. (2003). Stream temperature-equilibrium temperature  
707 relationship. *Water Resources Research*, 39(9), 1245. <https://doi.org/10.1029/2003WR002034>
- 708 Boudreault, J., Bergeron, N. E., St-Hilaire, A., & Chebana, F. (2019). Stream temperature  
709 modeling using functional regression models. *Journal of the American Water Resources*  
710 *Association*, 55(6), 1382–1400. <https://doi.org/10.1111/1752-1688.12778>
- 711 Boyd, M., and Kasper, B. (2003). Analytical methods for dynamic open channel heat and mass  
712 transfer: Methodology for Heat Source model version 7.0. Portland, OR: Oregon Department of  
713 Environmental Quality.
- 714 Brewitt, K. S., & Danner, E. M. (2014). Spatio-temporal temperature variation influences  
715 juvenile steelhead (*Oncorhynchus mykiss*) use of thermal refuges. *Ecosphere*, 5(7), art92.  
716 <https://doi.org/10.1890/ES14-00036.1>
- 717 Briggs, M. A., Johnson, Z. C., Snyder, C. D., Hitt, N. P., Kurylyk, B. L., Lautz, L., Irvine, D. J.,  
718 Hurley, S. T., & Lane, J. W. (2018). Inferring watershed hydraulics and cold-water habitat  
719 persistence using multi-year air and stream temperature signals. *Science of The Total*  
720 *Environment*, 636, 1117–1127. <https://doi.org/10.1016/j.scitotenv.2018.04.344>
- 721 Brown, G. W. (1969). Predicting temperatures of small streams. *Water Resources Research*,  
722 5(1), 68–75. <https://doi.org/10.1029/WR005i001p00068>
- 723 Cade, B. S., & Noon, B. R. (2003). A gentle introduction to quantile regression for ecologists.  
724 *Frontiers in Ecology and the Environment*, 1(8), 412–420. [https://doi.org/10.1890/1540-9295\(2003\)001\[0412:AGITQR\]2.0.CO;2](https://doi.org/10.1890/1540-9295(2003)001[0412:AGITQR]2.0.CO;2)
- 725
- 726 Caissie, D. (2006). The thermal regime of rivers: A review. *Freshwater Biology*, 51(8), 1389–  
727 1406. <https://doi.org/10.1111/j.1365-2427.2006.01597.x>
- 728 Caissie, D., El-Jabi, N., & Satish, M. G. (2001). Modelling of maximum daily water  
729 temperatures in a small stream using air temperatures. *Journal of Hydrology*, 251(1), 14–28.  
730 [https://doi.org/10.1016/S0022-1694\(01\)00427-9](https://doi.org/10.1016/S0022-1694(01)00427-9)
- 731 Caldwell, R. J., Gangopadhyay, S., Bountry, J., Lai, Y., & Elsner, M. M. (2013). Statistical  
732 modeling of daily and subdaily stream temperatures: Application to the Methow River Basin,  
733 Washington. *Water Resources Research*, 49(7), 4346–4361. <https://doi.org/10.1002/wrcr.20353>

- 734 CDFW (California Department of Fish and Wildlife) (2017). Interim Instream Flow Criteria for  
735 the Protection of Fishery Resources in the Scott River Watershed, Siskiyou County.  
736 [https://web.archive.org/web/20210324204650if\\_/https://nrm.dfg.ca.gov/FileHandler.ashx?Docu](https://web.archive.org/web/20210324204650if_/https://nrm.dfg.ca.gov/FileHandler.ashx?DocumentID=143476)  
737 [mentID=143476](https://web.archive.org/web/20210324204650if_/https://nrm.dfg.ca.gov/FileHandler.ashx?DocumentID=143476).
- 738 Chandesaris, A., Van Looy, K., Diamond, J. S., & Souchon, Y. (2019). Small dams alter thermal  
739 regimes of downstream water. *Hydrology and Earth System Sciences*, 23(11), 4509–4525.  
740 <https://doi.org/10.5194/hess-23-4509-2019>
- 741 Cline, T. J., Schindler, D. E., Walsworth, T. E., French, D. W., & Lisi, P. J. (2020). Low  
742 snowpack reduces thermal response diversity among streams across a landscape. *Limnology and*  
743 *Oceanography Letters*, 5(3), 254–263. <https://doi.org/10.1002/lol2.10148>.
- 744 Coleman, D., Bevitt, R., & Reinfelds, I. (2021). Predicting the thermal regime change of a  
745 regulated snowmelt river using a generalised additive model and analogue reference streams.  
746 *Environmental Processes*, 8(2), 511–531. <https://doi.org/10.1007/s40710-021-00501-7>
- 747 Crozier, L. G., Siegel, J. E., Wiesebron, L. E., Trujillo, E. M., Burke, B. J., Sandford, B. P., &  
748 Widener, D. L. (2020). Snake River sockeye and Chinook salmon in a changing climate:  
749 Implications for upstream migration survival during recent extreme and future climates. *PLOS*  
750 *ONE*, 15(9), e0238886. <https://doi.org/10.1371/journal.pone.0238886>
- 751 Dahlke, H., Brown, A., Orloff, S., Putnam, D., & O’Geen, T. (2018). Managed winter flooding  
752 of alfalfa recharges groundwater with minimal crop damage. *California Agriculture*, 72(1), 1–11.  
753 <https://doi.org/10.3733/ca.2018a0001>
- 754 Daly, C., Halbleib, M., Smith, J. I., Gibson, W. P., Doggett, M. K., Taylor, G. H., Curtis, J., &  
755 Pasteris, P. P. (2008). Physiographically sensitive mapping of climatological temperature and  
756 precipitation across the conterminous United States. *International Journal of Climatology*,  
757 28(15), 2031–2064. <https://doi.org/10.1002/joc.1688>
- 758 David, A. T., Asarian, J. E., & Lake, F. K. (2018). Wildfire smoke cools summer river and  
759 stream water temperatures. *Water Resources Research*, 54(10), 7273–7290.  
760 <https://doi.org/10.1029/2018WR022964>
- 761 Drake, D., Tate, K., & Carlson, H. (2000). Analysis shows climate-caused decreases in Scott  
762 River fall flows. *California Agriculture*, 54(6), 46–49. <https://doi.org/10.3733/ca.v054n06p46>
- 763 Dugdale, S. J., Hannah, D. M., & Malcolm, I. A. (2017). River temperature modelling: A review  
764 of process-based approaches and future directions. *Earth-Science Reviews*, 175, 97–113.  
765 <https://doi.org/10.1016/j.earscirev.2017.10.009>
- 766 Dugdale, S. J., Malcolm, I. A., Kantola, K., & Hannah, D. M. (2018). Stream temperature under  
767 contrasting riparian forest cover: Understanding thermal dynamics and heat exchange processes.  
768 *Science of The Total Environment*, 610–611, 1375–1389.  
769 <https://doi.org/10.1016/j.scitotenv.2017.08.198>
- 770 Dunham, J., Chandler, G., Rieman, B., Martin, D. (2005). Measuring stream temperature with  
771 digital data loggers: A user’s guide (*USDA Forest Service Gen. Tech. Rep. RMRS-GTR-*  
772 *150WWW*). [http://www.fs.fed.us/rm/pubs/rmrs\\_gtr150.pdf](http://www.fs.fed.us/rm/pubs/rmrs_gtr150.pdf)
- 773 Dymond, J. R. (1984). Water temperature change caused by abstraction. *Journal of Hydraulic*  
774 *Engineering*, 110(7), 987–991. [https://doi.org/10.1061/\(ASCE\)0733-9429\(1984\)110:7\(987\)](https://doi.org/10.1061/(ASCE)0733-9429(1984)110:7(987))

- 775 Fasiolo, M., Wood, S. N., Zaffran, M., Nedellec, R., & Goude, Y. (2020). Fast calibrated  
776 additive quantile regression. *Journal of the American Statistical Association*, 1–11.  
777 <https://doi.org/10.1080/01621459.2020.1725521>
- 778 Ficklin, D. L., Barnhart, B. L., Knouft, J. H., Stewart, I. T., Maurer, E. P., Letsinger, S. L., &  
779 Whittaker, G. W. (2014). Climate change and stream temperature projections in the Columbia  
780 River basin: Habitat implications of spatial variation in hydrologic drivers. *Hydrology and Earth  
781 System Sciences*, 18(12), 4897–4912. <https://doi.org/10.5194/hess-18-4897-2014>
- 782 FitzGerald, A. M., John, S. N., Apgar, T. M., Mantua, N. J., & Martin, B. T. (2021). Quantifying  
783 thermal exposure for migratory riverine species: Phenology of Chinook salmon populations  
784 predicts thermal stress. *Global Change Biology*, 27(3), 536–549.  
785 <https://doi.org/10.1111/gcb.15450>
- 786 Foglia, L., McNally, A., & Harter, T. (2013). Coupling a spatiotemporally distributed soil water  
787 budget with stream-depletion functions to inform stakeholder-driven management of  
788 groundwater-dependent ecosystems. *Water Resources Research*, 49(11), 7292–7310.  
789 <https://doi.org/10.1002/wrcr.20555>
- 790 Foglia, L., Neumann, J., Tolley, D., Orloff, S., Snyder, R., & Harter, T. (2018). Modeling guides  
791 groundwater management in a basin with river–aquifer interactions. *California Agriculture*,  
792 72(1), 84–95. <https://doi.org/10.3733/ca.2018a0011>
- 793 Folegot, S., Hannah, D. M., Dugdale, S. J., Kurz, M. J., Drummond, J. D., Klaar, M. J., Lee-  
794 Cullin, J., Keller, T., Martí, E., Zarnetske, J. P., Ward, A. S., & Krause, S. (2018). Low flow  
795 controls on stream thermal dynamics. *Limnologia*, 68, 157–167.  
796 <https://doi.org/10.1016/j.limno.2017.08.003>
- 797 Fullerton, A. H., Torgersen, C. E., Lawler, J. J., Faux, R. N., Steel, E. A., Beechie, T. J.,  
798 Ebersole, J. L., & Leibowitz, S. G. (2015). Rethinking the longitudinal stream temperature  
799 paradigm: Region-wide comparison of thermal infrared imagery reveals unexpected complexity  
800 of river temperatures. *Hydrological Processes*, 29(22), 4719–4737.  
801 <https://doi.org/10.1002/hyp.10506>
- 802 Gibeau, P., & Palen, W. J. (2020). Predicted effects of flow diversion by run-of-river  
803 hydropower on bypassed stream temperature and bioenergetics of salmonid fishes. *River  
804 Research and Applications*, 36(9), 1903–1915. <https://doi.org/10.1002/rra.3706>
- 805 Georges, B., Michez, A., Latte, N., Lejeune, P., & Brostaux, Y. (2021). Water stream heating  
806 dynamics around extreme temperature events: An innovative method combining GAM and  
807 differential equations. *Journal of Hydrology*, 601, 126600.  
808 <https://doi.org/10.1016/j.jhydrol.2021.126600>
- 809 Glover, R. S., Soulsby, C., Fryer, R. J., Birkel, C., & Malcolm, I. A. (2020). Quantifying the  
810 relative importance of stock level, river temperature and discharge on the abundance of juvenile  
811 Atlantic salmon (*Salmo salar*). *Ecohydrology*, 13(6), e2231. <https://doi.org/10.1002/eco.2231>
- 812 Gu, R. R., & Li, Y. (2002). River temperature sensitivity to hydraulic and meteorological  
813 parameters. *Journal of Environmental Management*, 66(1), 43–56.  
814 <https://doi.org/10.1006/jema.2002.0565>

- 815 Gu, R., Montgomery, S., & Austin, T. A. (1998). Quantifying the effects of stream discharge on  
816 summer river temperature. *Hydrological Sciences Journal*, 43(6), 885–904.  
817 <https://doi.org/10.1080/02626669809492185>
- 818 Hannah, D. M., Malcolm, I. A., & Bradley, C. (2009). Seasonal hyporheic temperature dynamics  
819 over riffle bedforms. *Hydrological Processes*, 23(15), 2178–2194.  
820 <https://doi.org/10.1002/hyp.7256>
- 821 Imholt, C., Gibbins, C. N., Malcolm, I. A., Langan, S., & Soulsby, C. (2010). Influence of  
822 riparian cover on stream temperatures and the growth of the mayfly *Baetis rhodani* in an upland  
823 stream. *Aquatic Ecology*, 44(4), 669–678. <https://doi.org/10.1007/s10452-009-9305-0>
- 824 Isaak, D. J., Luce, C. H., Horan, D. L., Chandler, G. L., Wollrab, S. P., Dubois, W. B., & Nagel,  
825 D. E. (2020). Thermal regimes of perennial rivers and streams in the Western United States.  
826 *Journal of the American Water Resources Association*, 1752-1688.12864.  
827 <https://doi.org/10.1111/1752-1688.12864>
- 828 Isaak, D. J., Luce, C. H., Horan, D. L., Chandler, G. L., Wollrab, S. P., & Nagel, D. E. (2018).  
829 Global warming of salmon and trout rivers in the Northwestern U.S.: Road to ruin or path  
830 through purgatory? *Transactions of the American Fisheries Society*, 147(3), 566–587.  
831 <https://doi.org/10.1002/tafs.10059>
- 832 Isaak, D. J., Wenger, S. J., Peterson, E. E., Hoef, J. M. V., Nagel, D. E., Luce, C. H., Hostetler,  
833 S. W., Dunham, J. B., Roper, B. B., Wollrab, S. P., Chandler, G. L., Horan, D. L., & Parkes-  
834 Payne, S. (2017). The NorWeST summer stream temperature model and scenarios for the  
835 Western U.S.: A crowd-sourced database and new geospatial tools foster a user community and  
836 predict broad climate warming of rivers and streams. *Water Resources Research*, 53(11), 9181–  
837 9205. <https://doi.org/10.1002/2017WR020969>
- 838 Islam, S. U., Hay, R. W., Déry, S. J., & Booth, B. P. (2019). Modelling the impacts of climate  
839 change on riverine thermal regimes in western Canada’s largest Pacific watershed. *Scientific*  
840 *Reports*, 9, 11398. <https://doi.org/10.1038/s41598-019-47804-2>
- 841 Jackson, F. L., Fryer, R. J., Hannah, D. M., Millar, C. P., & Malcolm, I. A. (2018). A spatio-  
842 temporal statistical model of maximum daily river temperatures to inform the management of  
843 Scotland’s Atlantic salmon rivers under climate change. *Science of The Total Environment*, 612,  
844 1543–1558. <https://doi.org/10.1016/j.scitotenv.2017.09.010>
- 845 Johnson, S. L. (2004). Factors influencing stream temperatures in small streams: Substrate  
846 effects and a shading experiment. *Canadian Journal of Fisheries and Aquatic Sciences*, 61(6),  
847 913–923.
- 848 Johnson, Z. C., Johnson, B. G., Briggs, M. A., Snyder, C. D., Hitt, N. P., & Devine, W. D.  
849 (2021). Heed the data gap: Guidelines for using incomplete datasets in annual stream  
850 temperature analyses. *Ecological Indicators*, 122, 107229.  
851 <https://doi.org/10.1016/j.ecolind.2020.107229>
- 852 Kelleher, C., Wagener, T., Gooseff, M., McGlynn, B., McGuire, K., & Marshall, L. (2012).  
853 Investigating controls on the thermal sensitivity of Pennsylvania streams. *Hydrological*  
854 *Processes*, 26(5), 771–785. <https://doi.org/10.1002/hyp.8186>

- 855 Kim, J.-S., & Jain, S. (2010). High-resolution streamflow trend analysis applicable to annual  
856 decision calendars: A western United States case study. *Climatic Change*, 102(3–4), 699–707.  
857 <https://doi.org/10.1007/s10584-010-9933-3>
- 858 KNF (Klamath National Forest) (2010). Klamath National Forest Sediment and Temperature  
859 Monitoring Plan and Quality Assurance Project Plan. Yreka, CA: Klamath National Forest.  
860 [https://web.archive.org/web/http://www.waterboards.ca.gov/water\\_issues/programs/tmdl/records](https://web.archive.org/web/http://www.waterboards.ca.gov/water_issues/programs/tmdl/records/region_1/2013/ref4082.pdf)  
861 [/region\\_1/2013/ref4082.pdf](https://web.archive.org/web/http://www.waterboards.ca.gov/water_issues/programs/tmdl/records/region_1/2013/ref4082.pdf).
- 862 KNF (Klamath National Forest) (2011). Klamath National Forest, Water and Air Temperature  
863 Monitoring Protocol, May 2011. Yreka, CA: Klamath National Forest.
- 864 Klemeš, V. (1986). Operational testing of hydrological simulation models. *Hydrological*  
865 *Sciences Journal*, 31(1), 13–24. <https://doi.org/10.1080/02626668609491024>
- 866 Klos, P. Z., Link, T. E., & Abatzoglou, J. T. (2014). Extent of the rain-snow transition zone in  
867 the western U.S. under historic and projected climate. *Geophysical Research Letters*, 41(13),  
868 4560–4568. <https://doi.org/10.1002/2014GL060500>
- 869 Koch, H., & Grünewald, U. (2010). Regression models for daily stream temperature simulation:  
870 Case studies for the river Elbe, Germany. *Hydrological Processes*, 24(26), 3826–3836.  
871 <https://doi.org/10.1002/hyp.7814>
- 872 Kurylyk, B. L., MacQuarrie, K. T. B., Linnansaari, T., Cunjak, R. A., & Curry, R. A. (2015).  
873 Preserving, augmenting, and creating cold-water thermal refugia in rivers: Concepts derived  
874 from research on the Miramichi River, New Brunswick (Canada). *Ecohydrology*, 8(6), 1095–  
875 1108. <https://doi.org/10.1002/eco.1566>
- 876 Laanaya, F., St-Hilaire, A., & Gloaguen, E. (2017). Water temperature modelling: Comparison  
877 between the generalized additive model, logistic, residuals regression and linear regression  
878 models. *Hydrological Sciences Journal*, 62(7), 1078–1093.  
879 <https://doi.org/10.1080/02626667.2016.1246799>
- 880 Leach, J. A., & Moore, R. D. (2019). Empirical stream thermal sensitivities may underestimate  
881 stream temperature response to climate warming. *Water Resources Research*, 55(7), 5453–5467.  
882 <https://doi.org/10.1029/2018WR024236>
- 883 Lee, S.-Y., Fullerton, A. H., Sun, N., & Torgersen, C. E. (2020). Projecting spatiotemporally  
884 explicit effects of climate change on stream temperature: A model comparison and implications  
885 for coldwater fishes. *Journal of Hydrology*, 588, 125066.  
886 <https://doi.org/10.1016/j.jhydrol.2020.125066>
- 887 Letcher, B. H., Hocking, D. J., O’Neil, K., Whiteley, A. R., Nislow, K. H., & O’Donnell, M. J.  
888 (2016). A hierarchical model of daily stream temperature using air-water temperature  
889 synchronization, autocorrelation, and time lags. *PeerJ*, 4, e1727.  
890 <https://doi.org/10.7717/peerj.1727>
- 891 Li, H., Deng, X., Kim, D.-Y., & Smith, E. P. (2014). Modeling maximum daily temperature  
892 using a varying coefficient regression model. *Water Resources Research*, 50(4), 3073–3087.  
893 <https://doi.org/10.1002/2013WR014243>

- 894 Luce, C., Staab, B., Kramer, M., Wenger, S., Isaak, D., & McConnell, C. (2014). Sensitivity of  
895 summer stream temperatures to climate variability in the Pacific Northwest. *Water Resources*  
896 *Research*, 50(4), 3428–3443. <https://doi.org/10.1002/2013WR014329>
- 897 Luo, Y., Ficklin, D. L., Liu, X., & Zhang, M. (2013). Assessment of climate change impacts on  
898 hydrology and water quality with a watershed modeling approach. *Science of The Total*  
899 *Environment*, 450–451, 72–82. <https://doi.org/10.1016/j.scitotenv.2013.02.004>
- 900 Lute, A. C., & Luce, C. H. (2017). Are model transferability and complexity antithetical?  
901 Insights from validation of a variable-complexity empirical snow model in space and time. *Water*  
902 *Resources Research*, 53(11), 8825–8850. <https://doi.org/10.1002/2017WR020752>
- 903 Manhard, C. V., N. A. Som, E. C. Jones, & R. W. Perry. 2018. Estimation of stream conditions  
904 in tributaries of the Klamath River, Northern California (*Arcata Fisheries Technical Report*  
905 *Number TR 2018-32*). Arcata, CA: U.S. Fish and Wildlife Service.  
906 [https://web.archive.org/web/https://www.fws.gov/arcata/fisheries/reports/technical/2018/Estimati](https://web.archive.org/web/https://www.fws.gov/arcata/fisheries/reports/technical/2018/EstimationofStreamConditionsinTributariesoftheKlamathRiverNorthernCalifornia.pdf)  
907 [onofStreamConditionsinTributariesoftheKlamathRiverNorthernCalifornia.pdf](https://web.archive.org/web/https://www.fws.gov/arcata/fisheries/reports/technical/2018/EstimationofStreamConditionsinTributariesoftheKlamathRiverNorthernCalifornia.pdf)
- 908 Mayer, T. D. (2012). Controls of summer stream temperature in the Pacific Northwest. *Journal*  
909 *of Hydrology*, 475(0), 323–335. <https://doi.org/10.1016/j.jhydrol.2012.10.012>
- 910 Meier, W., Bonjour, C., Wüest, A., & Reichert, P. (2003). Modeling the effect of water diversion  
911 on the temperature of mountain streams. *Journal of Environmental Engineering*, 129(8), 755–  
912 764. [https://doi.org/10.1061/\(ASCE\)0733-9372\(2003\)129:8\(755\)](https://doi.org/10.1061/(ASCE)0733-9372(2003)129:8(755))
- 913 Mierau, D. W., Trush, W. J., Rossi, G. J., Carah, J. K., Clifford, M. O., & Howard, J. K. (2017).  
914 Managing diversions in unregulated streams using a modified percent-of-flow approach.  
915 *Freshwater Biology*. <https://doi.org/10.1111/fwb.12985>
- 916 Mohseni, O., & Stefan, H. G. (1999). Stream temperature/air temperature relationship: A  
917 physical interpretation. *Journal of Hydrology*, 218(3), 128–141. [https://doi.org/10.1016/S0022-](https://doi.org/10.1016/S0022-1694(99)00034-7)  
918 [1694\(99\)00034-7](https://doi.org/10.1016/S0022-1694(99)00034-7)
- 919 Mohseni, O., Stefan, H. G., & Erickson, T. R. (1998). A nonlinear regression model for weekly  
920 stream temperatures. *Water Resources Research*, 34(10), 2685–2692.  
921 <https://doi.org/10.1029/98WR01877>
- 922 Moore, R. D., Spittlehouse, D. L., & Story, A. (2005). Riparian microclimate and stream  
923 temperature response to forest harvesting: A review. *Journal of the American Water Resources*  
924 *Association*, 41(4), 813–834. <https://doi.org/10.1111/j.1752-1688.2005.tb03772.x>
- 925 Neumann David W., Rajagopalan Balaji, & Zagona Edith A. (2003). Regression model for daily  
926 maximum stream temperature. *Journal of Environmental Engineering*, 129(7), 667–674.  
927 [https://doi.org/10.1061/\(ASCE\)0733-9372\(2003\)129:7\(667\)](https://doi.org/10.1061/(ASCE)0733-9372(2003)129:7(667))
- 928 Nichols, A. L., Willis, A. D., Jeffres, C. A., & Deas, M. L. (2014). Water temperature patterns  
929 below large groundwater springs: management implications for coho salmon in the Shasta River,  
930 California. *River Research and Applications*, 30(4), 442–455. <https://doi.org/10.1002/rra.2655>
- 931 NCRWQCB (North Coast Regional Water Quality Control Board) (2005). *Staff Report for the*  
932 *Action Plan for the Scott River Watershed Sediment and Temperature Total Maximum Daily*  
933 *Loads*. Santa Rosa, CA: North Coast Regional Water Quality Control Board.  
934 [https://www.waterboards.ca.gov/northcoast/water\\_issues/programs/tmdls/scott\\_river/staff\\_report](https://www.waterboards.ca.gov/northcoast/water_issues/programs/tmdls/scott_river/staff_report)

- 935 Null, S. E., Mouzon, N. R., & Elmore, L. R. (2017). Dissolved oxygen, stream temperature, and  
936 fish habitat response to environmental water purchases. *Journal of Environmental Management*,  
937 197, 559–570. <https://doi.org/10.1016/j.jenvman.2017.04.016>
- 938 Null, S. E., Viers, J. H., Deas, M. L., Tanaka, S. K., & Mount, J. F. (2013). Stream temperature  
939 sensitivity to climate warming in California's Sierra Nevada: Impacts to coldwater habitat.  
940 *Climatic Change*, 116(1), 149–170. <https://doi.org/10.1007/s10584-012-0459-8>
- 941 Ouellet, V., St-Hilaire, A., Dugdale, S. J., Hannah, D. M., Krause, S., & Proulx-Ouellet, S.  
942 (2020). River temperature research and practice: Recent challenges and emerging opportunities  
943 for managing thermal habitat conditions in stream ecosystems. *Science of The Total*  
944 *Environment*, 736, 139679. <https://doi.org/10.1016/j.scitotenv.2020.139679>
- 945 Pedersen, E. J., Miller, D. L., Simpson, G. L., & Ross, N. (2019). Hierarchical generalized  
946 additive models in ecology: An introduction with mgcv. *PeerJ*, 7, e6876.  
947 <https://doi.org/10.7717/peerj.6876>
- 948 Persad, G. G., Swain, D. L., Kouba, C., & Ortiz-Partida, J. P. (2020). Inter-model agreement on  
949 projected shifts in California hydroclimate characteristics critical to water management. *Climatic*  
950 *Change*. <https://doi.org/10.1007/s10584-020-02882-4>
- 951 Piotrowski, A. P., & Napiorkowski, J. J. (2019). Simple modifications of the nonlinear  
952 regression stream temperature model for daily data. *Journal of Hydrology*, 572, 308–328.  
953 <https://doi.org/10.1016/j.jhydrol.2019.02.035>
- 954 Poff, N. L., Tharme, R. E., & Arthington, A. H. (2017). Evolution of environmental flows  
955 assessment science, principles, and methodologies. In A. C. Horne, J. A. Webb, M. J.  
956 Stewardson, B. Richter, & M. Acreman (Eds.), *Water for the Environment* (pp. 203–236).  
957 Academic Press. <https://doi.org/10.1016/B978-0-12-803907-6.00011-5>
- 958 QVIR (Quartz Valley Indian Reservation) (2016). Quality assurance project plan 2016 revision  
959 water quality sampling and analysis, CWA 106 grant identification # I-96927206-0. Fort Jones,  
960 CA: QVIR Tribal Environmental Protection Department.
- 961 Railsback, S. F., Harvey, B. C., Kupferberg, S. J., Lang, M. M., McBain, S., & Welsh, H. H.  
962 (2016). Modeling potential river management conflicts between frogs and salmonids. *Canadian*  
963 *Journal of Fisheries and Aquatic Sciences*, 73(5), 773–784. <https://doi.org/10.1139/cjfas-2015-0267>
- 965 Roberts, D. R., Bahn, V., Ciuti, S., Boyce, M. S., Elith, J., Guillera-Arroita, G., Hauenstein, S.,  
966 Lahoz-Monfort, J. J., Schröder, B., Thuiller, W., Warton, D. I., Wintle, B. A., Hartig, F., &  
967 Dormann, C. F. (2017). Cross-validation strategies for data with temporal, spatial, hierarchical,  
968 or phylogenetic structure. *Ecography*, 40(8), 913–929. <https://doi.org/10.1111/ecog.02881>
- 969 Romberger, C. Z. and S. Gwozdz (2018). Performance of water temperature management on the  
970 Klamath and Trinity Rivers, 2017. (*U.S. Fish and Wildlife Service, Arcata Fisheries Data Series*  
971 *Number DS 2018-59*).
- 972 Santiago, J. M., Muñoz-Mas, R., Solana-Gutiérrez, J., García de Jalón, D., Alonso, C., Martínez-  
973 Capel, F., Pórtoles, J., Monjo, R., & Ribalaygua, J. (2017). Waning habitats due to climate  
974 change: The effects of changes in streamflow and temperature at the rear edge of the distribution  
975 of a cold-water fish. *Hydrology and Earth System Sciences*, 21(8), 4073–4101.  
976 <https://doi.org/10.5194/hess-21-4073-2017>

- 977 Shaw, S. B. (2017). Does an upper limit to river water temperature apply in all places?  
978 *Hydrological Processes*, 31(21), 3729–3739. <https://doi.org/10.1002/hyp.11297>
- 979 Siegel, J. E., & Volk, C. J. (2019). Accurate spatiotemporal predictions of daily stream  
980 temperature from statistical models accounting for interactions between climate and landscape.  
981 *PeerJ*, 7, e7892. <https://doi.org/10.7717/peerj.7892>
- 982 Sinokrot, B. A., & Gulliver, J. S. (2000). In-stream flow impact on river water temperatures.  
983 *Journal of Hydraulic Research*, 38(5), 339–349. <https://doi.org/10.1080/00221680009498315>
- 984 Sohrabi, M. M., Benjankar, R., Tonina, D., Wenger, S. J., & Isaak, D. J. (2017). Estimation of  
985 daily stream water temperatures with a Bayesian regression approach. *Hydrological Processes*,  
986 31(9), 1719–1733. <https://doi.org/10.1002/hyp.11139>
- 987 Smith, C. D., Rounds, S. A., & Orzol, L. L. (2018). Klamath River Basin water-quality data.  
988 (USGS Numbered Series *Fact Sheet* 2018–3031). <https://doi.org/10.3133/fs20183031>
- 989 Soto, B. (2016). Assessment of Trends in Stream Temperatures in the North of the Iberian  
990 Peninsula Using a Nonlinear Regression Model for the Period 1950–2013. *River Research and*  
991 *Applications*, 32(6), 1355–1364. <https://doi.org/10.1002/rra.2971>
- 992 Stanford, J.A. & Ward, J.V. (1992). Management of aquatic resources in large catchments:  
993 Recognizing interactions between ecosystem connectivity and environmental disturbance. In R.  
994 J. Naiman (Editor). *Watershed Management: Balancing Sustainability and Environmental*  
995 *Change* (pp. 91–124). New York, NY: Springer.
- 996 St-Hilaire, A., Boyer, C., Bergeron, N., & Daigle, A. (2018). Water temperature monitoring in  
997 Eastern Canada: A case study for network optimization. *WIT Transactions on Ecology and the*  
998 *Environment*, 228, 269–275. <https://doi.org/10.2495/WP180251>
- 999 Steel, E. A., Beechie, T. J., Torgersen, C. E., & Fullerton, A. H. (2017). Envisioning,  
1000 quantifying, and managing thermal regimes on river networks. *BioScience*, 67(6), 506–522.  
1001 <https://doi.org/10.1093/biosci/bix047>
- 1002 Superior Court of Siskiyou County (1980). Scott River adjudication, decree no. 30662. Scott  
1003 River stream system, Siskiyou County. Sacramento, CA: State Water Resources Control Board.
- 1004 Sutton, R. J., Deas, M. L., Tanaka, S. K., Soto, T., & Corum, R. A. (2007). Salmonid  
1005 observations at a Klamath River thermal refuge under various hydrological and meteorological  
1006 conditions. *River Research and Applications*, 23(7), 775–785.
- 1007 Sutton, R., & Soto, T. (2012). Juvenile coho salmon behavioural characteristics in Klamath river  
1008 summer thermal refugia. *River Research and Applications*. <https://doi.org/10.1002/rra.1459>
- 1009 Tague, C., Farrell, M., Grant, G., Lewis, S., & Rey, S. (2007). Hydrogeologic controls on  
1010 summer stream temperatures in the McKenzie River basin, Oregon. *Hydrological Processes*,  
1011 21(24), 3288–3300. <https://doi.org/10.1002/hyp.6538>
- 1012 Theurer, F.D., Voos, K.A., & Miller, W.J. (1984). Instream water temperature model. *Instream*  
1013 *Flow Information Paper 16*. FWS/OBS-84/15. Washington, D.C.: US Fish and Wildlife Service.
- 1014 Tolley, D., Foglia, L., & Harter, T. (2019). Sensitivity analysis and calibration of an integrated  
1015 hydrologic model in an irrigated agricultural basin with a groundwater-dependent ecosystem.  
1016 *Water Resources Research*, 55(9), 7876–7901. <https://doi.org/10.1029/2018WR024209>

- 1017 USEPA (U.S. Environmental Protection Agency) (2003). EPA Region 10 guidance for Pacific  
1018 Northwest state and tribal temperature water quality standards. EPA 910-B-03-002. Seattle, WA:  
1019 Region 10 Office of Water.
- 1020 Van Kirk, R. W., & Naman, S. W. (2008). Relative effects of climate and water use on base-flow  
1021 trends in the Lower Klamath Basin. *Journal of the American Water Resources Association*,  
1022 44(4), 1035–1052. <https://doi.org/10.1111/j.1752-1688.2008.00212.x>
- 1023 VanderKooi, S., Thorsteinson, L., & Clark, M. (2011). Environmental and historical setting. In  
1024 L. Thorsteinson, S. VanderKooi, & W. Duffy (Eds.), *Proceedings of the Klamath Basin Science*  
1025 *Conference*, Medford, Oregon, February 1–5, 2010 (pp. 31–36). Reston, VA: U.S. Geological  
1026 Survey.
- 1027 van Rij, J., Hendriks, P., van Rijn, H., Baayen, R. H., & Wood, S. N. (2019). Analyzing the time  
1028 course of pupillometric data. *Trends in Hearing*, 23, 233121651983248.  
1029 <https://doi.org/10.1177/2331216519832483>
- 1030 van Rij, J., Wieling, M., Baayen, R., van Rijn, H. (2020). itsadug: Interpreting time series and  
1031 autocorrelated data using GAMMs. *R package version 2.4*. [https://cran.r-](https://cran.r-project.org/package=itsadug)  
1032 [project.org/package=itsadug](https://cran.r-project.org/package=itsadug)
- 1033 van Vliet, M. T. H., Ludwig, F., Zwolsman, J. J. G., Weedon, G. P., & Kabat, P. (2011). Global  
1034 river temperatures and sensitivity to atmospheric warming and changes in river flow. *Water*  
1035 *Resources Research*, 47(2). <https://doi.org/10.1029/2010WR009198>
- 1036 Webb, B. W., Clack, P. D., & Walling, D. E. (2003). Water–air temperature relationships in a  
1037 Devon river system and the role of flow. *Hydrological Processes*, 17(15), 3069–3084.  
1038 <https://doi.org/10.1002/hyp.1280>
- 1039 Webb, B. W., Hannah, D. M., Moore, R. D., Brown, L. E., & Nobilis, F. (2008). Recent  
1040 advances in stream and river temperature research. *Hydrological Processes*, 22(7), 902–918.  
1041 <https://doi.org/10.1002/hyp.6994>
- 1042 Wenger, S. J., Isaak, D. J., Luce, C. H., Neville, H. M., Fausch, K. D., Dunham, J. B., Dauwalter,  
1043 D. C., Young, M. K., Elsner, M. M., Rieman, B. E., Hamlet, A. F., & Williams, J. E. (2011).  
1044 Flow regime, temperature, and biotic interactions drive differential declines of trout species  
1045 under climate change. *Proceedings of the National Academy of Sciences*, 108(34), 14175–14180.  
1046 <https://doi.org/10.1073/pnas.1103097108>
- 1047 Westerling, A. L. (2016). Increasing western US forest wildfire activity: Sensitivity to changes in  
1048 the timing of spring. *Philosophical Transactions of the Royal Society B: Biological Sciences*,  
1049 371(1696), 20150178. <https://doi.org/10.1098/rstb.2015.0178>
- 1050 Wood, S.N. (2017). *Generalized additive models: An introduction with R (2nd edition)*.  
1051 Chapman and Hall/CRC.
- 1052 Wrzesiński, D., & Graf, R. (2022). Temporal and spatial patterns of the river flow and water  
1053 temperature relations in Poland. *Journal of Hydrology and Hydromechanics*, 70(1), 12–29.  
1054 <https://doi.org/10.2478/johh-2021-0033>
- 1055 Yan, H., Sun, N., Fullerton, A., & Baerwalde, M. (2021). Greater vulnerability of snowmelt-fed  
1056 river thermal regimes to a warming climate. *Environmental Research Letters*, 16(5), 054006.  
1057 <https://doi.org/10.1088/1748-9326/abf393>

- 1058 Yang, G., & Moyer, D. L. (2020). Estimation of nonlinear water-quality trends in high-frequency  
1059 monitoring data. *Science of The Total Environment*, 715, 136686.  
1060 <https://doi.org/10.1016/j.scitotenv.2020.136686>
- 1061 Yard, M. D., Bennett, G. E., Mietz, S. N., Coggins, L. G., Stevens, L. E., Hueftle, S., & Blinn, D.  
1062 W. (2005). Influence of topographic complexity on solar insolation estimates for the Colorado  
1063 River, Grand Canyon, AZ. *Ecological Modelling*, 183(2), 157–172.  
1064 <https://doi.org/10.1016/j.ecolmodel.2004.07.027>
- 1065 Yarnell, S. M., Stein, E. D., Webb, J. A., Grantham, T., Lusardi, R. A., Zimmerman, J., Peek, R.  
1066 A., Lane, B. A., Howard, J., & Sandoval-Solis, S. (2020). A functional flows approach to  
1067 selecting ecologically relevant flow metrics for environmental flow applications. *River Research*  
1068 *and Applications*, rra.3575. <https://doi.org/10.1002/rra.3575>

1069

### 1070 **References From the Supporting Information**

- 1071 Daly, C., Doggett, M. K., Smith, J. I., Olson, K. V., Halbleib, M. D., Dimcovic, Z., Keon, D.,  
1072 Loiselle, R. A., Steinberg, B., Ryan, A. D., Pancake, C. M., & Kaspar, E. M. (2021). Challenges  
1073 in observation-based mapping of daily precipitation across the conterminous United States.  
1074 *Journal of Atmospheric and Oceanic Technology*, 38(11), 1979–1992.  
1075 <https://doi.org/10.1175/JTECH-D-21-0054.1>
- 1076 Lusardi, R. A., Hammock, B. G., Jeffres, C. A., Dahlgren, R. A., & Kiernan, J. D. (2019).  
1077 Oversummer growth and survival of juvenile coho salmon (*Oncorhynchus kisutch*) across a  
1078 natural gradient of stream water temperature and prey availability: An in situ enclosure  
1079 experiment. *Canadian Journal of Fisheries and Aquatic Sciences*, 1–12.  
1080 <https://doi.org/10.1139/cjfas-2018-0484>
- 1081 McGrath, E. O., Neumann, N. N., & Nichol, C. F. (2017). A statistical model for managing water  
1082 temperature in streams with anthropogenic influences. *River Research and Applications*, 33(1),  
1083 123–134. <https://doi.org/10.1002/rra.3057>
- 1084 Menne, M.J., Durre, I., Korzeniewski, B., McNeal, S., Thomas, K., Yin, X., Anthony, S., Ray,  
1085 R., Vose, R.S., Gleason, B.E., & Houston, T.G. (2012a). Global historical climatology network -  
1086 daily (GHCN-Daily), version 3.26. NOAA National Climatic Data Center.  
1087 <http://doi.org/10.7289/V5D21VHZ>. Accessed 2021-01-11
- 1088 Menne, M. J., Durre, I., Vose, R. S., Gleason, B. E., & Houston, T. G. (2012b). An overview of  
1089 the global historical climatology network-daily database. *Journal of Atmospheric and Oceanic*  
1090 *Technology*, 29(7), 897–910. <https://doi.org/10.1175/JTECH-D-11-00103.1>
- 1091 Moore, R. B., & Dewald, T. G. (2016). The road to NHDPlus—Advancements in digital stream  
1092 networks and associated catchments. *Journal of the American Water Resources Association*,  
1093 52(4), 890–900. <https://doi.org/10.1111/1752-1688.12389>
- 1094 Steel, E. A., Kennedy, M. C., Cunningham, P. G., & Stanovick, J. S. (2013). Applied statistics in  
1095 ecology: Common pitfalls and simple solutions. *Ecosphere*, 4(9), art115.  
1096 <https://doi.org/10.1890/ES13-00160.1>

- 1097 Stenhouse, S., Pisano, M., Bean, C., & Chesney, W. (2012). Water temperature thresholds for  
1098 coho salmon in a spring fed river, Siskiyou County, California. *California Fish and Game*, 98(1),  
1099 19–37.
- 1100 Welsh, H. H., Hodgson, G. R., Harvey, B. C., & Roche, M. F. (2001). Distribution of juvenile  
1101 coho salmon in relation to water temperatures in tributaries of the Mattole River, California.  
1102 *North American Journal of Fisheries Management*, 21(3), 464–470.  
1103 [https://doi.org/10.1577/1548-8675\(2001\)021<0464:DOJCSI>2.0.CO;2](https://doi.org/10.1577/1548-8675(2001)021<0464:DOJCSI>2.0.CO;2)
- 1104 Zillig, K. W., Lusardi, R. A., Moyle, P. B., & Fanguie, N. A. (2021). One size does not fit all:  
1105 Variation in thermal eco-physiology among Pacific salmonids. *Reviews in Fish Biology and*  
1106 *Fisheries*. <https://doi.org/10.1007/s11160-020-09632-w>  
1107

1108 **Figure 1.** Klamath Basin study sites with the Scott River Watershed outlined in red. Source map  
1109 credits: Esri , NOAA, and USGS.

1110

1111 **Figure 2.** Time series of (a) daily mean air temperature, (b) daily mean flow, (c) daily maximum  
1112 stream temperature ( $T_{\max}$ ), and (d) daily mean stream temperature ( $T_{\text{mean}}$ ) at Scott River from  
1113 1998–2020.

1114

1115 **Figure 3.** Inputs to Scott River “quantile air temperature” scenarios representing 15  
1116 combinations of (a) three air temperature inputs and (b) five flow inputs that vary by day.  
1117 Observed values for 1998–2020 are shown as gray lines.

1118

1119 **Figure 4.** Configuration of data blocks used in extrapolation tests for model selection and  
1120 validation.

1121

1122 **Figure 5.** Summary of RMSE from extrapolation and LOYO CV tests at 10 Klamath Basin sites  
1123 applying  $T_{\max}$  (top panels) and  $T_{\text{mean}}$  (bottom panels) models to years (LOYO) or flow and air  
1124 temperature combinations (extrapolation) not used in model calibration. Models are sorted by  
1125 overall RMSE (i.e., mean of all 10 sites and both temperature metrics). Data labels for top eight  
1126 models in individual site panels are means from extrapolation tests, with asterisk marking lowest  
1127 RMSE in each panel. Labels at right edge of graph are all-site means for each model and  
1128 parameter.

1129

1130 **Figure 6.** Effects of flow ( $Q$ ) and day of year ( $D$ ) on predicted values of (a)  $T_{\max}$  and (b)  $T_{\text{mean}}$  in  
1131 Scott River GAM7. Colors and labeled contour lines show predicted temperatures ( $^{\circ}\text{C}$ ).  
1132 Underlying gray dots show calibration data.

1133

1134 **Figure 7.** Modeled Scott River  $T_{\max}$  and  $T_{\text{mean}}$  under the 15 “quantile air temperature” scenarios  
1135 representing combinations of three air temperature inputs (arranged in columns) and three  
1136 quantile flow inputs and two management flow inputs (shown by color). Observed values for  
1137 1998–2020 are shown as gray lines. Selected data values are labeled on 15 June and the first day  
1138 of March–October. Horizontal dashed line is the salmonid temperature threshold.

1139

1140 **Figure 8.** Modeled stream temperature differences between lowest flow (0.1 quantile) and  
1141 highest flow (0.9 quantile) scenarios throughout the year for (a)  $T_{\max}$  and (b)  $T_{\text{mean}}$  at 10 Klamath  
1142 Basin sites estimated using GAM7.

1143

1144 **Figure 9.** (a) Annual maximum stream temperature, (b) annual degree-days exceeding  $22^{\circ}\text{C}$ ,  
1145 and (c) first and (d) last day when  $T_{\max}$  exceeded  $22^{\circ}\text{C}$  in Scott River model scenarios pairing  
1146 observed air temperatures with eight flow scenarios. Means of all years are shown with black  
1147 points and grey “x” show individual years, offset for clarity.

1148 **Table 1.** List of Scott River GAMs and model training statistics.  
1149

Model Name	Predictor variables	Daily maximum stream temperature ( $T_{\max}$ )						Daily mean stream temperature ( $T_{\text{mean}}$ )					
		BIC	AR1	edf <sub>F</sub>	edf <sub>R</sub>	RMSE	R <sup>2</sup>	BIC	AR1	edf <sub>F</sub>	edf <sub>R</sub>	RMSE	R <sup>2</sup>
GAM1: tensor Q- $A_{2w}$ -D	te(Q, $A_{2w}$ , D)	12830	0.526	23.6	18.1	1.06	0.973	8562	0.659	22.8	18.1	0.80	0.978
GAM2: tensors Q-D & $A_{2w}$ -D	s( $A_{2w}$ ) + ti( $A_{2w}$ , D) + te(Q, D)	12734	0.529	18.4	18.0	1.05	0.974	8492	0.667	17.1	18.0	0.80	0.979
GAM3: tensor Q-D & vary $A_{2w}$	s(D, by = $A_{2w}$ ) + s( $A_{2w}$ ) + te(Q, D)	12745	0.531	18.0	18.0	1.05	0.974	8482	0.672	16.3	18.0	0.80	0.978
GAM4: tensors Q-D & $A_{2w}$ -Q	s(D, by = $A_{2w}$ ) + s( $A_{2w}$ ) + ti( $A_{2w}$ , Q) + te(Q, D)	12717	0.531	17.2	17.9	1.05	0.974	8486	0.671	16.9	18.0	0.80	0.978
GAM5: tensor Q-D no vary $A_{2w}$	s( $A_{2w}$ ) + te(Q, D)	12724	0.537	15.7	17.9	1.06	0.974	8456	0.679	15.6	17.9	0.80	0.978
GAM6: vary Q & $A_{2w}$ linear	s(D, by = $A_{2w}$ ) + s(D, by = Q) + s(D)	12828	0.578	13.9	17.8	1.12	0.970	8594	0.728	10.9	17.3	0.89	0.973
GAM7: vary Q & $A_{2w}$ (final)	s(D, by = $A_{2w}$ ) + s( $A_{2w}$ ) + s(Q) + s(D, by = Q) + s(D)	12754	0.544	12.6	17.9	1.07	0.973	8538	0.695	11.8	17.6	0.84	0.976
GAM8: vary Q & no vary $A_{2w}$	s( $A_{2w}$ ) + s(Q) + s(D, by = Q) + s(D)	12736	0.552	12.3	17.8	1.08	0.973	8526	0.704	11.8	17.5	0.84	0.976
GAM9: $A_{2w}$ no vary	s( $A_{2w}$ ) + s(Q) + s(D)	13105	0.673	8.4	17.6	1.32	0.959	8738	0.764	8.1	17.6	0.96	0.969
GAM10: $A_{2w}$ no Q or vary	s( $A_{2w}$ ) + s(D)	13313	0.780	6.0	17.3	1.62	0.938	9150	0.840	6.0	16.6	1.20	0.952
GAM11: A7 only no AR1	s( $A_7$ )	22668	N/A	5.8	0	2.40	0.865	20265	N/A	5.8	0	1.88	0.882

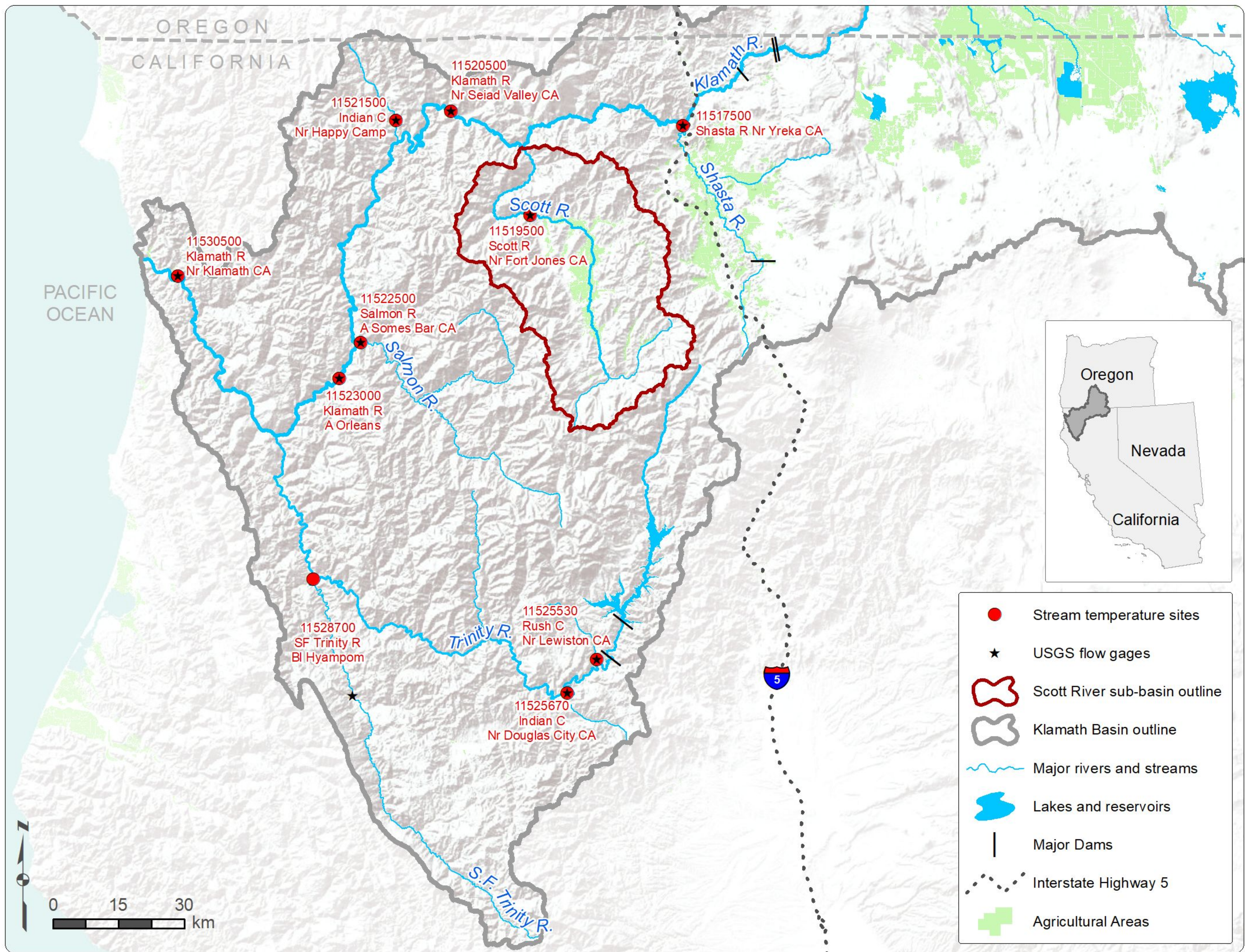
1150 *Note:* Models are sorted by edf<sub>F</sub> for  $T_{\max}$ , from most complex (GAM1) to least complex (GAM11). Except GAM11, all models also  
1151 include an AR1 autocorrelation structure and random effect of year. D = day of year from 1 (1 January) to 366 (31 December in leap  
1152 year), Q = daily mean flow, see Section 3.1.2 for key to ‘A’ air temperature variables, ‘s()’ is a nonlinear function, ‘s(D, by =)’ is a  
1153 linear interaction that varies smoothly by D, ‘te()’ is a fully nonlinear tensor product smooth of two or three variables, ‘ti()’ is a tensor  
1154 product interaction, BIC = Bayesian information criterion score, AR1 = autocorrelation coefficient, edf<sub>F</sub> = effective degrees of  
1155 freedom (edf) for fixed effects, edf<sub>R</sub> = edf for random effects, RMSE = root mean squared error of model training fit (not CV), and R<sup>2</sup>  
1156 = coefficient of determination from model training fit (not CV).

1157 **Table 2.** Matrix showing model scenarios representing combinations of air temperature and flow  
 1158 inputs, and organized into two scenario groups. The first group (15 scenarios) used “quantile air  
 1159 temperature” inputs (6 were only run only at Scott River while 9 were run at all Klamath Basin  
 1160 sites) and the second group (8 scenarios) were run only at Scott River and used “observed air  
 1161 temperature” inputs.  
 1162

Scenario group	Air temperature inputs	Flow inputs							
		Lowest (0.1 quantile)	Typical (0.5 quantile)	Highest (0.9 quantile)	USFS water right	CDFW flow criteria	Observed	Maximum of observed or USFS	Maximum of observed or CDFW
Quantile air temperature	Hottest (0.9 quantile)	All sites	All sites	All sites	Scott only	Scott only			
	Typical (0.5 quantile)	All sites	All sites	All sites	Scott only	Scott only			
	Coollest (0.1 quantile)	All sites	All sites	All sites	Scott only	Scott only			
Observed air temperature	Observed (measured on date)	Scott only	Scott only	Scott only	Scott only	Scott only	Scott only	Scott only	Scott only

1163

Figure 1.



- Stream temperature sites
- ★ USGS flow gages
- Scott River sub-basin outline
- Klamath Basin outline
- ~ Major rivers and streams
- Lakes and reservoirs
- | Major Dams
- ⋯ Interstate Highway 5
- + Agricultural Areas

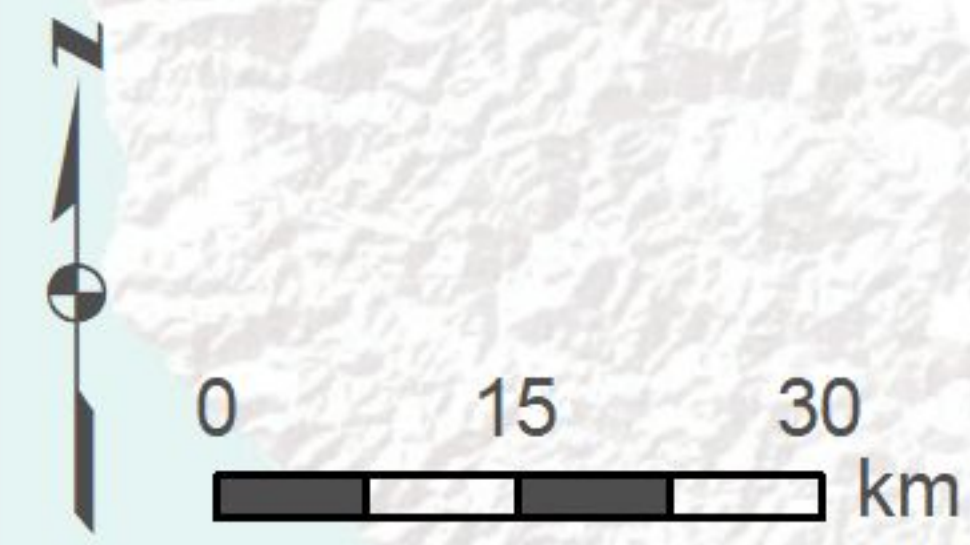


Figure 2.

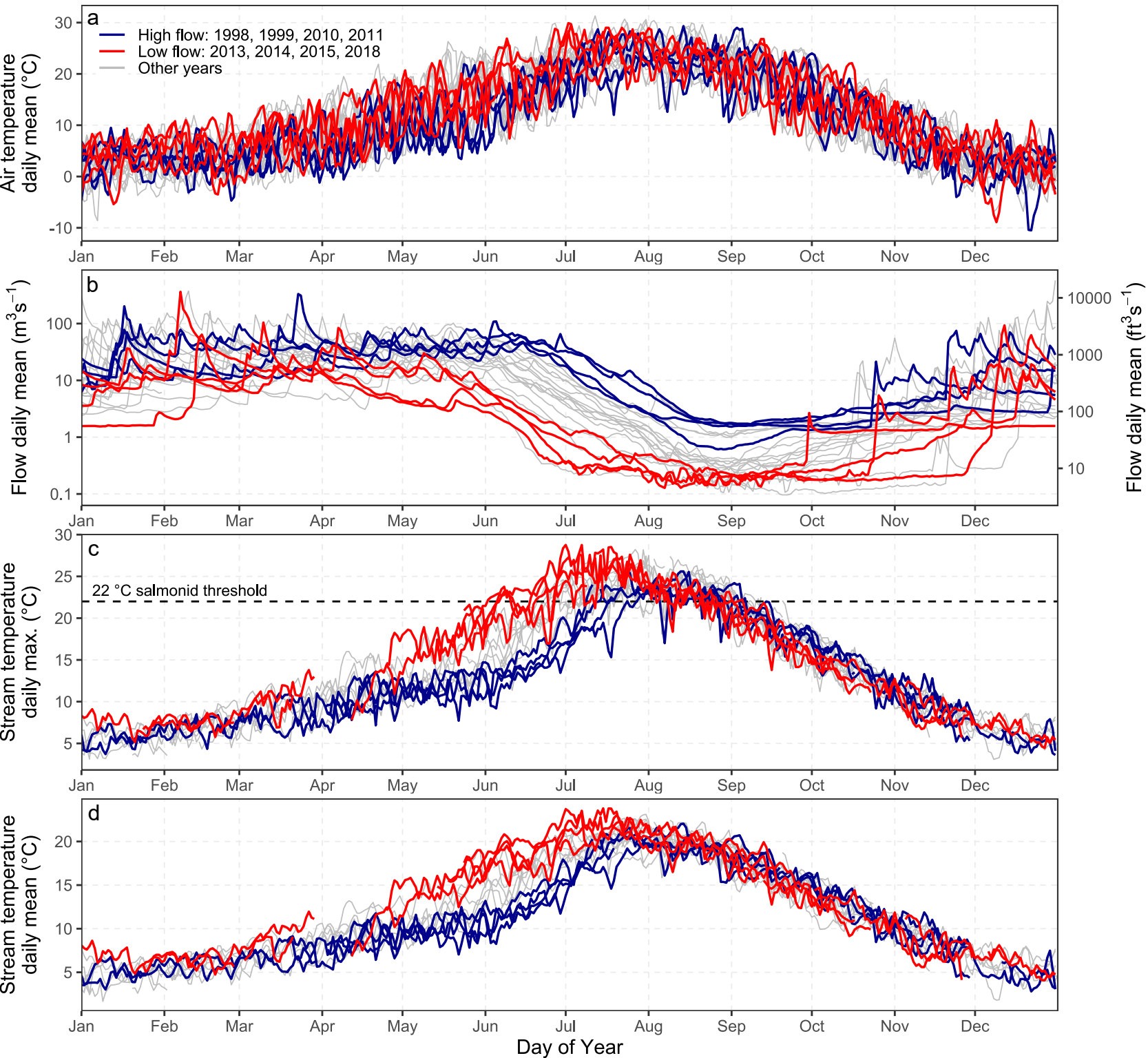


Figure 3.

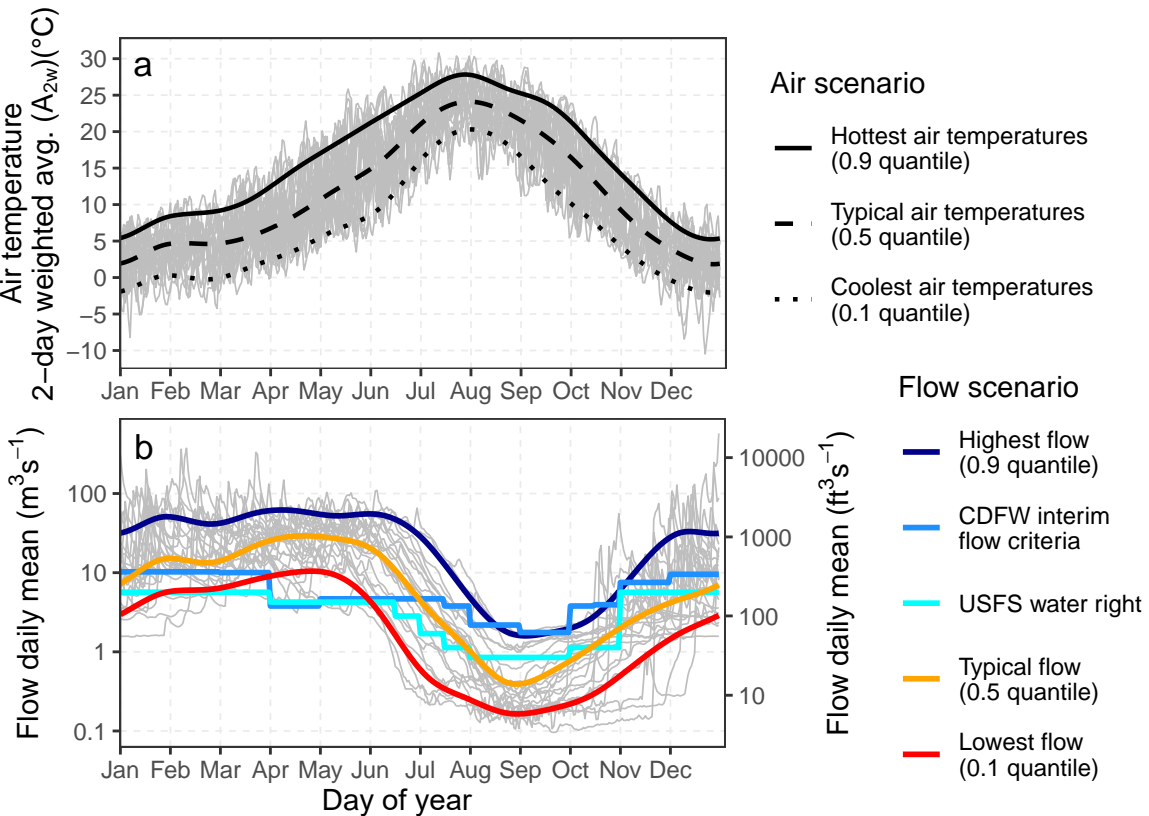
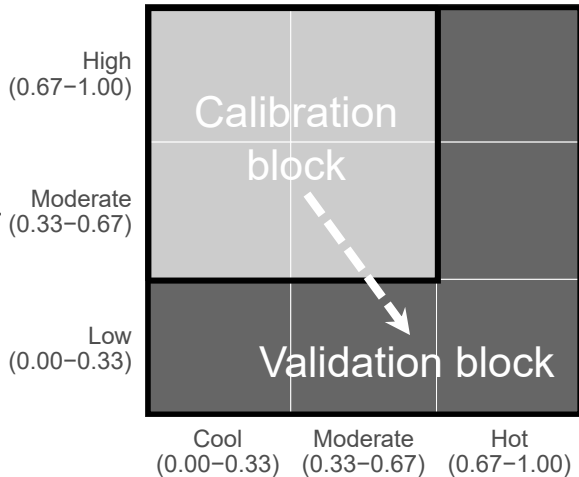
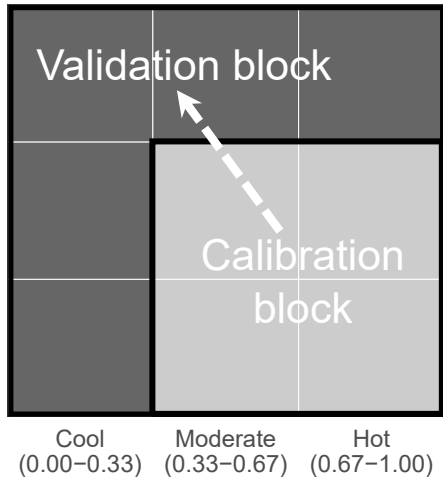


Figure 4.

Predict Low-flow and/or Warm days  
from  
High-flow, Moderate, and/or Cool days



Predict High-flow and/or Cool days  
from  
Low-flow, Moderate, and/or Warm days



Air temperature quantile

Figure 5.

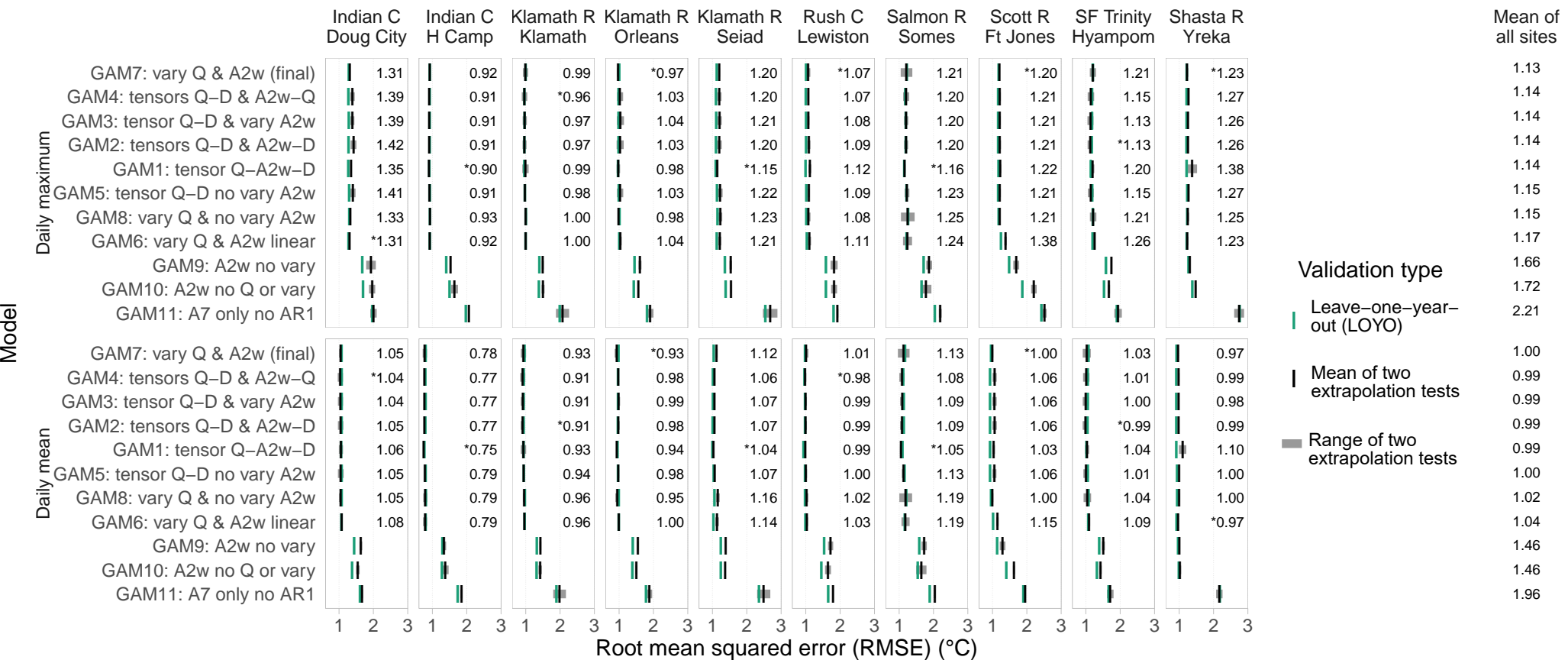


Figure 6.

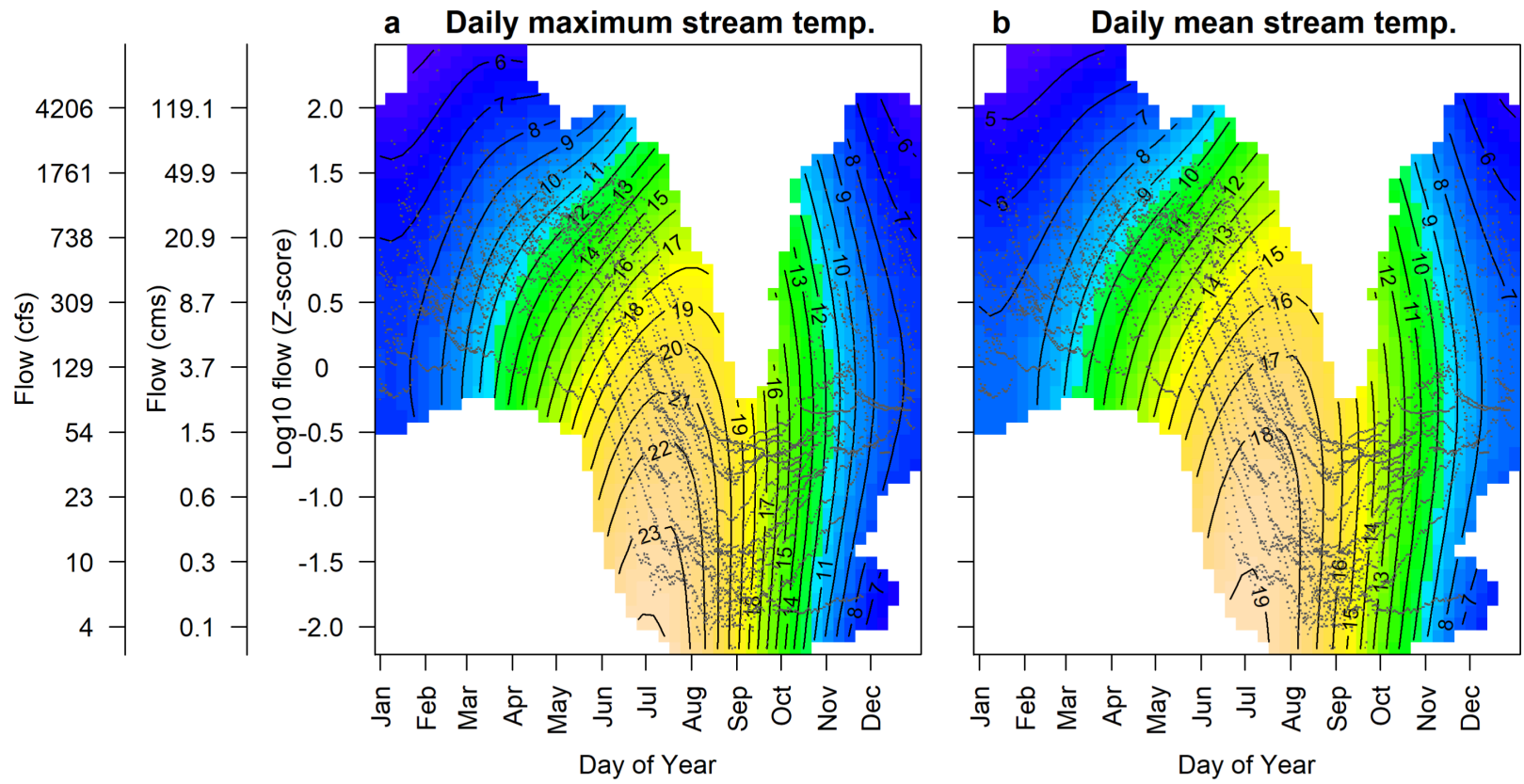


Figure 7.



Figure 8.

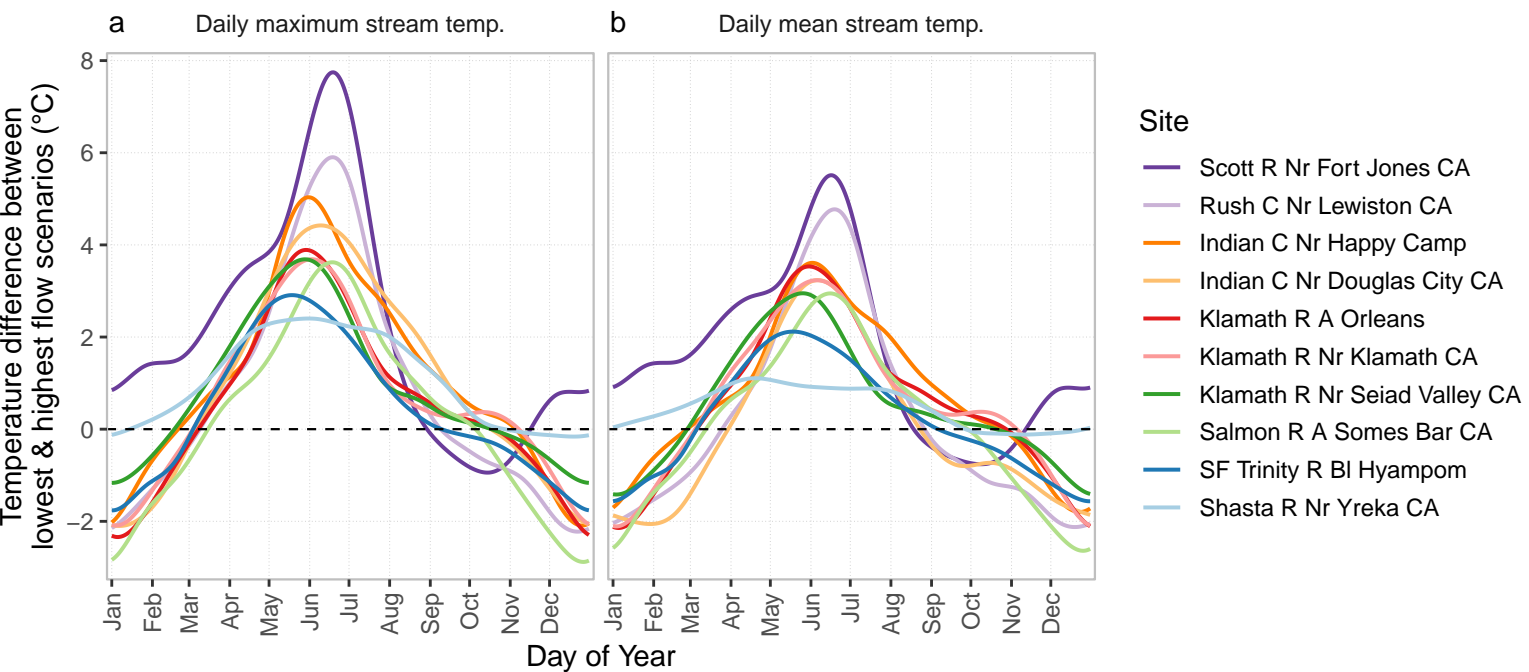


Figure 9.

